

RELAXATION MODELS FOR SCALAR TRAFFIC NETWORKS AND ZERO RELAXATION LIMIT

R. BORSCHÉ* AND A. KLAR*[†]

Abstract. In this paper we propose coupling conditions for a relaxation model for vehicular traffic on networks. We present a matched asymptotic expansion procedure to derive a LWR- network with well-known classical coupling conditions from the relaxation network in the macroscopic limit. Similar to the asymptotic limit of boundary value problems, we perform an asymptotic analysis of the interface layers at the nodes and a matching procedure using half-Riemann problems for the limit conservation law. Moreover, we present numerical experiments comparing the relaxation network with the LWR network for a broader range of coupling conditions.

1. Introduction. Modeling and simulation of traffic flow on road networks, has been investigated intensively using hyperbolic partial differential equations. Different models have been used, ranging from scalar conservation laws like the Lighthill Whitham Richards model through models using system of conservation laws, [41, 1, 8, 27, 26, 19, 20], to kinetic descriptions of the flow [27, 31, 33, 42, 21]. Derivations of these models from the underlying models in such hierarchies have been discussed as well, see, [2, 27, 34, 6], for a non-exhaustive list of references. To obtain a model for the dynamics on the full network, all these models have to be supplemented with coupling conditions at the nodes of the network. Coupling conditions for scalar conservation laws and systems of conservation laws on networks have been discussed in many papers, see, for example, [17, 13, 32, 24, 37, 14, 4, 15, 16, 22, 35]. Kinetic and relaxation equations on networks have been considered, for example, in [28, 12].

A procedure to derive coupling conditions for macroscopic equations from the underlying ones of the kinetic or relaxation equation has been discussed for linear systems in [11] using an asymptotic analysis of the situation near the nodes. A simple nonlinear case has been treated in [10]. To explain the general procedure in more detail, we consider a relaxation equation in 1D involving a scaling parameter ϵ , which converges for $\epsilon \rightarrow 0$ to an associated scalar conservation law for traffic flow. If such equations are considered on a network, it is sufficient to study a single coupling point or node, where coupling conditions are required. Suitable coupling conditions have to be imposed for the relaxation problem at each node. If ϵ is sent to zero, layers near the junctions can arise. To consider the limit $\epsilon \rightarrow 0$, one has to proceed similarly as in the case of boundary value problems, where a complete picture of the convergence is only obtained, once boundary- and initial layers are investigated. We refer to [5, 7, 25, 43] for such a procedure for boundary value problems in the case of kinetic equations and to [46, 44, 38, 45] for the case of hyperbolic relaxation systems.

In the present work, we consider the case of a relaxation system on a network with a small parameter ϵ leading in the limit $\epsilon \rightarrow 0$ to a LWR-type scalar conservation law. Besides the definition of suitable coupling conditions for the relaxation system at the junction, the present work aims at presenting a matched asymptotic expansion procedure leading from the relaxation model on the network to the scalar conservation law. Analytical, as well as numerical investigations are presented.

Based on the discussion of the Riemann problems at the nodes we propose coupling conditions for the relaxation model for merging and diverging junctions. These

[†]Technische Universität Kaiserslautern, Department of Mathematics, Erwin-Schrödinger-Straße, 67663 Kaiserslautern, Germany ({borsche, klar}@mathematik.uni-kl.de)

^{*}Fraunhofer ITWM, Fraunhoferplatz 1, 67663 Kaiserslautern, Germany

conditions are developed in a similar way as those for other well-known higher order traffic models like the ARZ-equations, see [29]. However, due to the simpler structure of the relaxation model compared to the ARZ-equations, the conditions are much easier to handle and to investigate and allow a relatively straightforward asymptotic derivation of classical coupling conditions for the LWR-type traffic equations in the limit ϵ going to 0. Moreover, in the case of diverging junctions the coupling conditions defined here guarantee that the coupled solution of the two-equation model remain in the physically reasonable state-space domain defined by bounds on density and velocity in contrast to coupling conditions for the ARZ-model discussed in the literature [29, 35] and references therein.

The asymptotic procedure gives a detailed account of the situation near the node in the case of small values of the relaxation parameter ϵ . Besides the structure of the layers near the nodes and the coupling conditions for the limit problem, it reveals, that the effective densities for the relaxation system at the node for small ϵ are not necessarily the same as those found by the coupling conditions for the relaxation system.

The paper is organized in the following way. In section 2 we present the relaxation model, compare [9], and the associated scalar conservation law. In section 3 different coupling conditions for the relaxation model for merging and diverging junctions are discussed and the associated Riemann problems at the nodes are investigated. Moreover, the associated classical coupling conditions for the limiting scalar conservation law are stated. In section 4 the asymptotic procedure and the matched asymptotic expansion on the network is explained together with a discussion of the layer solutions of the relaxation system. Then, the asymptotic procedure is investigated in detail analytically in section 5. There, it is shown that a special merge conditions for the relaxation system leads in the relaxation limit to a classical merge condition for the nonlinear scalar conservation law. Finally, the solutions of the relaxation system on the network are compared numerically to the solution of the scalar conservation law on the network in section 6 for the case of merging and diverging junctions and a broader range of coupling conditions.

2. Relaxation model and scalar traffic equations. Consider the LWR-traffic flow equations

$$\partial_t \rho + \partial_x F(\rho) = 0, \quad (2.1)$$

where $F = F(\rho)$ is a given traffic density-flow function or fundamental diagram, i.e. a smooth function $F : [0, 1] \rightarrow [0, 1]$ with $F(0) = 0 = F(1)$ and $F'(\rho) \leq 1$. In the following we restrict ourselves to strictly concave fundamental diagrams F , where the point, where the maximum of F is attained, is denoted by ρ^* and the maximal value is $F(\rho^*) = \sigma$.

We are interested in the investigation of relaxation systems for the LWR equations on networks. The minimal requirements of such a relaxation system for the density ρ and the flux q are the convergence towards the LWR-equations and the invariance of the 'traffic domain' given by $0 \leq \rho \leq 1$ and $0 \leq q \leq \rho$. This is the physically reasonable state-space for a 2x2 traffic equation, see e.g. [8]. The above two conditions correspond to an upper bound on the density $\rho_{max} = 1$ and an upper bound to the velocity $v = q/\rho$ given by v_{max} .

A simple example is given by the following relaxation system [9] for the LWR equations for the variables density ρ and flux q , which we will use as a prototype for

the discussion of the issues mentioned in the introduction. The equations are

$$\begin{aligned} \partial_t \rho + \partial_x q &= 0 \\ \partial_t q + \frac{q}{1-\rho} \partial_x \rho + \left(1 - \frac{q}{1-\rho}\right) \partial_x q &= -\frac{1}{\epsilon} (q - F(\rho)) . \end{aligned} \quad (2.2)$$

This is a hyperbolic system with the eigenvalues $\lambda_1 = -\frac{q}{1-\rho} \leq 0 < \lambda_2 = 1$. The respective eigenvectors are $r_1 = (1, \lambda_1)^T$, $r_2 = (1, 1)$. A straightforward computation shows that the r_1 - and the r_2 -field are both linearly degenerate. The system is totally linear degenerate (TLD). The integral curves (and shock curves) of the hyperbolic system are given by $q = q_L \frac{1-\rho}{1-\rho_L}$ for the 1-field and by $q = \rho - \rho_R + q_R$ for the 2-field. The region $0 \leq \rho \leq 1, 0 \leq q \leq \rho$ is an invariant region for the relaxation system as it is easily seen by considering the integral curves, see Figure 2.1. We refer to [9] for details and for a kinetic interpretation of the equations. Note that the fact, that the system is TLD strongly simplifies the calculations and leads in many situations to explicitly computable quantities and conditions.

The equations can be rewritten in conservative form choosing the variable $z = \frac{q}{1-\rho}$. Rewriting (2.2) we obtain

$$\begin{aligned} \partial_t \rho + \partial_x q &= 0 \\ \partial_t z + \partial_x z &= -\frac{1}{\epsilon} (z - Z(\rho)) \end{aligned} \quad (2.3)$$

with $q = z(1-\rho)$ and $Z(\rho) = \frac{F(\rho)}{1-\rho}$. A Riemann invariant of the first characteristic family is obviously

$$z = \frac{q}{1-\rho} \in [0, \infty) .$$

A Riemann invariant of the second characteristic family is

$$w = \rho - q \in [0, 1] .$$

Concerning the convergence of its solutions towards the solutions of the scalar conservation law $\partial_t \rho + \partial_x F(\rho) = 0$ as ϵ tends to 0 the subcharacteristic condition has to be satisfied [38]. Setting $q = F(\rho)$ in the formula for the eigenvalues, the subcharacteristic condition states

$$-\frac{F(\rho)}{1-\rho} \leq F'(\rho) \leq 1 \quad \text{for } 0 \leq \rho \leq 1 .$$

REMARK 1. *The condition is fulfilled for strictly concave fundamental diagrams F . For example, in the classical LWR case with $F(\rho) = \rho(1-\rho)$ and $F'(\rho) = 1-2\rho$ the above condition is*

$$-\rho \leq 1-2\rho \leq 1 \quad \text{for } 0 \leq \rho \leq 1 ,$$

which is obviously satisfied.

Finally we note that boundary conditions for the relaxation system (2.2) on the interval $[x_L, x_R]$ have to be prescribed in the following way. Since the first eigenvalue is always non-positive and the second is a positive constant, the number of boundary conditions is fixed. At the left boundary at $x = x_L$ we have to prescribe a value

for the 1-Riemann invariant $z(x_L) = \frac{q(x_L)}{1-\rho(x_L)}$. For the right boundary $x = x_R$ the 2-Riemann invariant $w(x_R) = \rho(x_R) - q(x_R)$ has to be prescribed.

REMARK 2. Compare the present model with the ARZ model [1]

$$\begin{aligned} \partial_t \rho + \partial_x q &= 0 \\ \partial_t q + \frac{q}{\rho} \left(\rho p'(\rho) - \frac{q}{\rho} \right) \partial_x \rho + \left(\frac{q}{\rho} + \frac{q}{\rho} - \rho p'(\rho) \right) \partial_x q &= -\frac{1}{\epsilon} (q - F(\rho)). \end{aligned} \quad (2.4)$$

or in conservative form

$$\begin{aligned} \partial_t \rho + \partial_x q &= 0 \\ \partial_t (\rho z_R) + \partial_x (q z_R) &= -\frac{1}{\epsilon} (q - F(\rho)). \end{aligned} \quad (2.5)$$

with $q = \rho z_R - \rho p(\rho)$. We note that the above domain $0 \leq \rho \leq 1$ and $0 \leq q \leq \rho$ is also an invariant domain for the ARZ conditions, if p is appropriately chosen with a singularity at $\rho = 1$, see [8].

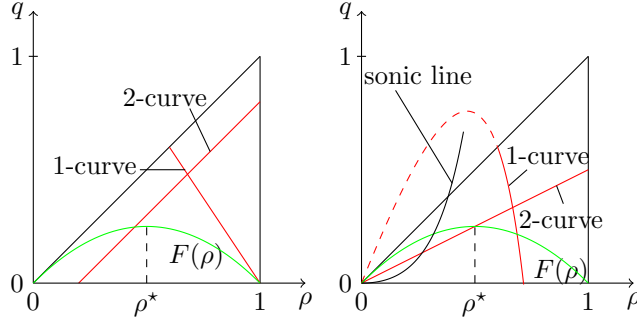


Fig. 2.1: Lax-curves in (ρ, q) variables for the totally degenerate relaxation system (left figure) and the ARZ equations with $p(\rho) = \frac{\rho}{1-\rho}$ (right figure).

3. Coupling conditions for the relaxation system on networks and associated conditions for the LWR equations. In this section we propose general coupling conditions for the relaxation model (2.2) for different physical situations. As long as appropriate we will proceed in a similar way as in [23, 29] for the definition of the coupling conditions for the ARZ-model. At the same time we state classical coupling conditions for these situations for the LWR equations. In section 5 the coupling conditions for the relaxation system will be related via a matched asymptotic expansion procedure to the coupling conditions for the LWR model on networks. There, we consider the case of a merging junction with a special merge condition analytically. The other cases will be investigated numerically in section 6. We restrict ourselves here to the case of junctions with either two ingoing and one outgoing lane (merging junction) or a junction with two outgoing and one ingoing lane (diverging junction), see Figure 3.1.

As on each road, there is exactly one outgoing characteristic family for the relaxation system, we have to provide three conditions at a junction connecting three roads. We denote the quantities at the junctions by $\rho^i, q^i, i = 1, 2, 3$ and the corresponding Riemann invariants by z^i, w^i . In any case the conservation of mass will be

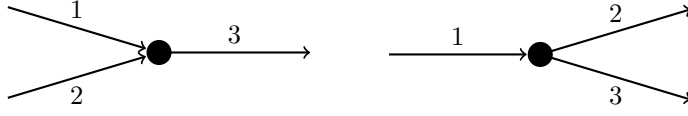


Fig. 3.1: On the left: A junction with two ingoing and one outgoing road (2-1 node). On the right: A junction with one incoming and two outgoing roads (1-2 node).

imposed, i.e. all cars entering a junction via one of the incoming roads will exit on the outgoing road. The other two conditions depend on the physical situation under consideration. We consider first the case of a 2-1 node.

3.1. Merging lanes. In this case the Riemann invariants z^1, z^2, w^3 are prescribed and the admissible states at the junction in (ρ, q) -plane fulfill

$$\begin{aligned} q^1 &= z^1(1 - \rho^1) \\ q^2 &= z^2(1 - \rho^2) \\ q^3 &= \rho^3 - w^3. \end{aligned} \tag{3.1}$$

The coupling conditions are the balance of fluxes

$$q^1 + q^2 = q^3 \tag{3.2}$$

and a relation for the Riemann invariants for the first characteristic family z (which is also the momentum flux of the conservative variable). For merging junctions, one might simply choose the balance of z , i.e. $z^3 = z^1 + z^2$ or more general

$$z^3 = g(z^1, z^2, w^3) \tag{3.3}$$

with some function g . We use as a simple example $g = z^1 + z^2$ for the investigations in section 5 and 6 and also for the illustrations in Figures 3.2 and 3.3.

REMARK 3. Compare [29] for the corresponding balance condition of the momentum flux for the ARZ-equations

$$q^3 z_R^3 = q^1 z_R^1 + q^2 z_R^2.$$

Note that this condition is required to obtain weak solutions on the network in the sense of [32]. The condition $z^3 = z^1 + z^2$ is the analogue to this condition for the equations considered here.

To continue, one more relation is needed to solve the Riemann problem at the junction uniquely. We consider two approaches. The first approach assumes a relation of the incoming fluxes given by the prescribed quantities z^1, z^2, w^3 . That means, additionally to 3.2 and 3.3 we consider the general condition

$$\frac{q^1}{q^2} = f \tag{3.4}$$

with $f = f(z^1, z^2, w^3)$ or equivalently

$$\begin{aligned} q^1 &= \frac{f}{1+f} q^3 \\ q^2 &= \frac{1}{1+f} q^3. \end{aligned} \quad (3.5)$$

As an example, we use simply

$$f = \frac{z^1}{z^2}, \quad (3.6)$$

that means, that the relation between q^1 and q^2 is given by the relation of the corresponding Riemann invariants.

The second, more general approach describes a lane merging via a condition on the flux q^1 . We prescribe a relation

$$q^1 = F(q^3; z^1, z^2, w^3) \leq \rho^1. \quad (3.7)$$

For example, for a merging with a priority lane, here lane 1, we consider additionally to the conditions 3.2 and 3.3, the following condition on the flux q^1

$$q^1 = \min\{q^3, \rho^1\}. \quad (3.8)$$

This can be rewritten as

$$q^1 = \bar{q}^1 \quad (3.9)$$

with $\bar{q}^1 = \min(q^3, q^{max}(z^1))$, where the maximal possible flux for the Riemann invariant z is defined as $q^{max}(z) = \frac{z}{1+z}$.

A more general condition giving a partial priority to one of the roads depending on a value $P \in [0, 1]$ is given by a convex combination of the priority conditions for lane 1 and 2, i.e.

$$q^1 = (1 - P)\bar{q}^1 + P(q^3 - \bar{q}^2) \quad (3.10)$$

See e.g. [35] for a partial priority merging condition for the ARZ equations.

This leads to a distribution depending on the maximal possible fluxes on the two ingoing roads as long as the maximal flux given by q^3 is not exceeded and to a distribution according to the priority value P , if both maximal possible fluxes are larger than q^3 . For the symmetric case $P = \frac{1}{2}$ we obtain

$$q^1 = \frac{1}{2} (q^3 + \bar{q}^1 - \bar{q}^2) \quad (3.11)$$

which is easily seen to be equivalent to

$$q^1 = \min\left(\bar{q}^1, q^3 - \min(\bar{q}^1, \bar{q}^2, \frac{q^3}{2})\right). \quad (3.12)$$

See Figure 3.4 for the proportion $\frac{q^1}{q^3}$ of the flux in lane 1 for z^2 ranging from 0 to 0.5.

All these conditions lead to a well-posed Riemann problem at the junction. This can be easily seen by solving the problems explicitly.

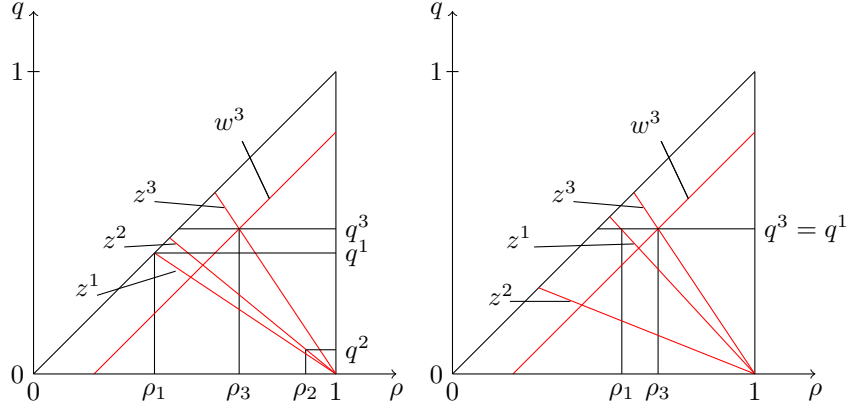


Fig. 3.3: Solution of Riemann problems for junction with priority lane. On the left $\frac{z^1}{1+z^1} \leq q^3$. On the right $\frac{z^1}{1+z^1} \geq q^3$.

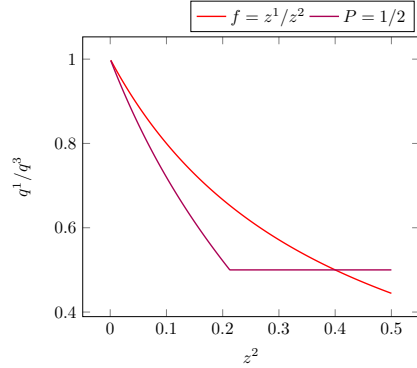


Fig. 3.4: Proportion $\frac{q^1}{q^3}$ of the flux in lane 1 for $z^2 \in [0, 0.5]$ and $z^1 = 0.4$. Coupling conditions (3.6) and (3.11) are shown.

For the outgoing road $i = 3$

$$\rho_B^i \leq \rho^* \Rightarrow \Omega^i = [0, \sigma] \quad \text{and} \quad \rho_B^i \geq \rho^* \Rightarrow \Omega^i = [0, F(\rho_B^i)].$$

We define the maximal admissible flux c^i such that $\Omega^i = [0, c^i]$.

The coupling conditions are in both cases given by the balance of fluxes $C^3 = C^1 + C^2$. Moreover, for $c^1 + c^2 \leq c^3$ the conditions

$$C^1 = c^1, C^2 = c^2$$

are used. For $c^1 + c^2 \geq c^3$ we have the 'fair merging' conditions

$$C^i = \min \left(c^i, c^3 - \min \left(c^1, c^2, \frac{c^3}{2} \right) \right), \quad i = 1, 2 \quad (3.15)$$

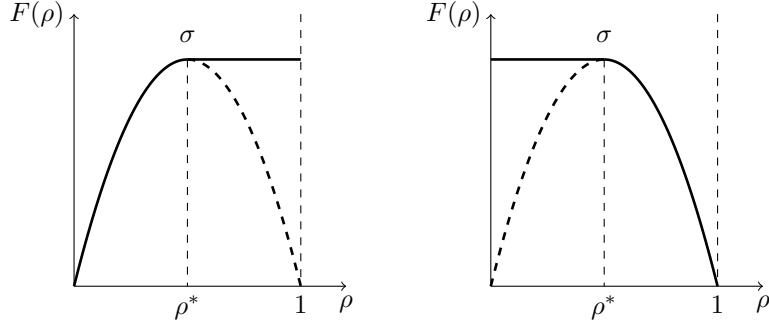


Fig. 3.5: Supply- and demand functions c^i for ingoing (left) and outgoing (right) roads.

and in the case, where lane 1 is a priority lane,

$$\begin{aligned}
 C^1 &= \min(c^1, c^3) \\
 C^2 &= c^3 - C^1 = \max(c^3 - c^1, 0).
 \end{aligned}
 \tag{3.16}$$

REMARK 4. *That means, in the 'fair merging' case the merging is symmetric, if both incoming roads have a flux which is larger than their share in the outgoing road. We refer, for example, to [24] for such coupling conditions for LWR networks.*

In sections 5 and 6 we consider the limit of the above coupling conditions for the relaxation system as $\epsilon \rightarrow 0$ analytically and numerically. In section 5 an analytical investigation of the asymptotic procedure is given for conditions (3.6) and it is shown that the LWR condition (3.15) is obtained in the limit as ϵ goes to 0. The numerical experiments in Section 6 show that the macroscopic fair merging conditions (3.15) are obtained not only from conditions (3.6), but also, for example, from condition (3.11), which is less surprising comparing (3.12) and (3.11). There is obviously a larger range of conditions on the level of the relaxation system leading to the macroscopic conditions (3.15). We note that the coupling condition for the relaxation system modelling a priority lane (3.8) leads to the corresponding macroscopic condition (3.16).

3.2. Diverging lanes. In this case the quantities z^1, w^2, w^3 are given at the junction and the admissible states fulfill

$$\begin{aligned}
 q^1 &= z^1(1 - \rho^1) \\
 q^2 &= \rho^2 - w^2 \\
 q^3 &= \rho^3 - w^3.
 \end{aligned}
 \tag{3.17}$$

Again, the coupling conditions contain in all cases the balance of fluxes

$$q^1 = q^2 + q^3. \tag{3.18}$$

To ensure that the resulting values at the junction remain in the physical domain $0 \leq \rho \leq 1, 0 \leq q \leq \rho$, we choose q^1 as

$$q^1 = \min\{\bar{q}, \rho^1\}.$$

where \bar{q} is determined such that a prescribed relation

$$z^1 = g(z^2, z^3) \quad (3.19)$$

is fulfilled.

EXAMPLE 2. *As an example we use, in Figures 3.6 and 3.7 and in the numerical experiments, the function $g = z^2 + z^3$. Note that in this case the balance of the momentum flux is only fulfilled as long as this condition leads to values inside the domain $0 \leq \rho \leq 1, 0 \leq q \leq \rho$. For a more detailed discussion, see Section 3.3.*

Additionally, either the relation of the outgoing fluxes is prescribed, i.e.

$$\frac{q^2}{q^3} = f \quad (3.20)$$

with $f = f(w^2, w^3, z^1) \in \mathbb{R}_+$, which is equivalent to

$$q^2 = \frac{f}{1+f}q^1, \quad q^3 = \frac{1}{1+f}q^1. \quad (3.21)$$

Or we use an additive relation

$$q^2 - q^3 = f \quad (3.22)$$

with $f = f(w^2, w^3, z^1) \in [-1, 1]$. (3.22) can be rewritten as

$$q^2 = \frac{q^1}{2} + \frac{f}{2} \text{ and } q^3 = \frac{q^1}{2} - \frac{f}{2}. \quad (3.23)$$

REMARK 5. *In the first case, typically, one prescribes a fixed relation*

$$f = \frac{\alpha}{1-\alpha}, \quad (3.24)$$

where $\alpha \in [0, 1]$ is given by the drivers preferences to go to one of the roads. This can be rewritten as

$$q^2 = \alpha q^1 \text{ and } q^3 = (1-\alpha)q^1. \quad (3.25)$$

As an example for the function f in the second case, we use

$$f = w^3 - w^2. \quad (3.26)$$

Such a relation describes a distribution of the outgoing fluxes adapted to the situation in the outgoing roads without drivers preferences.

For a comparison of these conditions with the ARZ equations, as given for example in [29], see section 3.3.

Again we discuss the explicit solutions of the Riemann problems at the junction.

3.2.1. Solution of the Riemann problems. In the first case, we determine q^1 as

$$q^1 = \min\left\{\frac{z^1}{1+z^1}, \bar{q}\right\}$$

where \bar{q} is determined by solving (in general numerically) the equation

$$z^1 = g \left(\frac{f\bar{q}}{(1-w^2)(1+f) - f\bar{q}}, \frac{\bar{q}}{(1-w^3)(1+f) - \bar{q}} \right), \quad (3.27)$$

which is assumed to have a unique solution $q \geq 0$ in a range, such that $\rho^2 = w^2 + \frac{f}{1+f}\bar{q}$ and $\rho_3 = w^3 + \frac{1}{1+f}\bar{q}$ are in $[0, 1]$.

Then q^2 and q^3 are obtained straightforwardly. This yields finally ρ^1, ρ^2 and ρ^3 due to the characteristic equations.

EXAMPLE 3. For example, for $g = z^2 + z^3$ and $f = 1$, i.e. $\alpha = \frac{1}{2}$ and $w^2 = \bar{w} = w^3$ we have explicitly for $\bar{w} \geq \frac{z^1}{2(1+z^1)}$

$$q^1 = \bar{q} = \frac{2z^1}{2+z^1}(1-\bar{w})$$

and $\rho^1 = \rho^2 = \rho^3$. For $\bar{w} \leq \frac{z^1}{2(1+z^1)}$ we have $q^1 = \rho^1 = \frac{z^1}{1+z^1}$ and $\rho^2 = \rho^3$. See Figure 3.6 for an illustration in phase-space. Note that for g as before, but general $\alpha \in [0, 1]$ and $w^2, w^3 \in [0, 1]$, equation (3.27) is equivalent to the quadratic equation

$$z^1(a - \bar{q})(b - \bar{q}) = \bar{q}((a + b) - 2\bar{q})$$

with $a = \frac{1-w^2}{\alpha}, b = \frac{1-w^3}{1-\alpha}$. This equation is easily seen to have a unique solution in the range $0 \leq \bar{q} \leq \min(a, b)$, which is equivalent to $\rho^2 = w^2 + \alpha\bar{q}$ and $\rho^3 = w^3 + (1-\alpha)\bar{q}$ in $[0, 1]$.

For the second relation in Section 3.2, i.e. for (3.22) we have

$$q^1 = \min\left\{\frac{z^1}{1+z^1}, \bar{q}\right\},$$

where \bar{q} is determined from the equation

$$z^1 = g \left(\frac{\bar{q} + f}{2(1-\rho^2)}, \frac{\bar{q} - f}{2(1-\rho^3)} \right)$$

with $\rho^2 = q^2 + w^2 = \frac{\bar{q}+f}{2} + w^2$ and $\rho^3 = q^3 + w^3 = \frac{\bar{q}-f}{2} + w^3$. Again the equation is assumed to have a unique solution $q \geq 0$ such that ρ^1 and ρ^2 above are in $[0, 1]$. The remaining quantities are obtained in a straightforward way.

EXAMPLE 4. Using $g = z^1 + z^2$ and $f = w^3 - w^2$ we have always $\rho^2 = \rho^3 = \bar{\rho}$. Moreover, \bar{q} is now determined from

$$z^1 = \frac{\bar{q} + w^3 - w^2}{2(1-\rho^2)} + \frac{\bar{q} - w^3 + w^2}{2(1-\rho^3)} = \frac{\bar{q}}{1 - \frac{\bar{q}}{2} - \frac{w^2+w^3}{2}}.$$

This is explicitly solved and we obtain for $w^2 + w^3 \geq \frac{z^1}{1+z^1}$

$$q^1 = \bar{q} = (2 - (w^2 + w^3)) \frac{z^1}{2 + z^1}$$

and

$$\rho^1 = \rho^2 = \rho^3 = \frac{w^2 + w^3 + z^1}{2 + z^1}.$$

For $w^2 + w^3 \leq \frac{z^1}{1+z^1}$ we obtain $q^1 = \frac{z^1}{1+z^1}$ and $\rho^2 = \rho^3 = \frac{z^1 + (1+z^1)(w^2+w^3)}{2(1+z^1)}$. See Figure 3.7 for the illustration of these conditions.

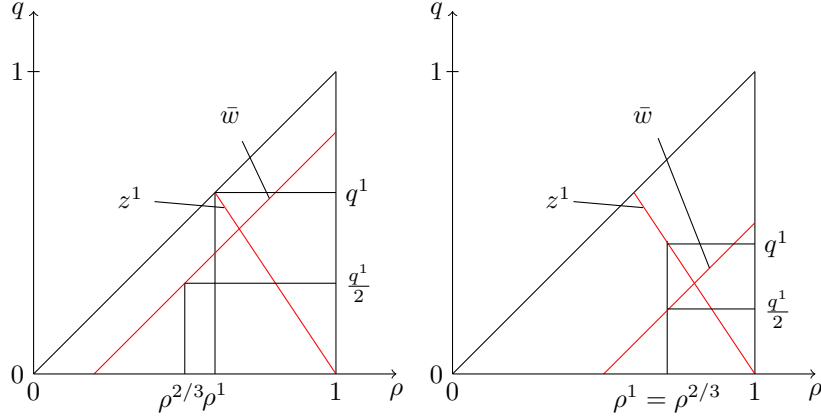


Fig. 3.6: Solution of Riemann problems for diverging junction with drivers preferences, $\bar{w} = w^2 = w^3, \alpha = \frac{1}{2}$. On the left $\frac{z^1}{2(1+z^1)} \geq \bar{w}$. On the right $\frac{z^1}{2(1+z^1)} \leq \bar{w}$.

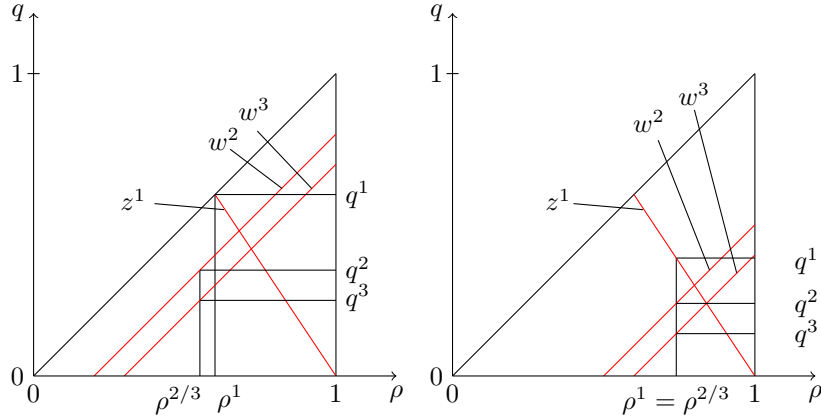


Fig. 3.7: Solution of Riemann problems for diverging junction without driver preferences. On the left $\frac{z^1}{1+z^1} \geq w^2 + w^3$. On the right $\frac{z^1}{1+z^1} \leq w^2 + w^3$.

3.2.2. LWR-conditions. Classical coupling conditions for the LWR network for the two diverging situations are well known, see [24]. Using the notation from Section 3.1.2 we always have $C^1 = C^2 + C^3$. Additionally, we have for the situation with driver preferences

$$C^1 = \min\left(c^1, \frac{1}{\alpha}c^2, \frac{1}{1-\alpha}c^3\right) \quad (3.28)$$

and

$$\frac{C^2}{C^3} = \frac{\alpha}{1-\alpha}. \quad (3.29)$$

Without drivers preferences the additional conditions are for $c^2 + c^3 \leq c^1$

$$C^2 = c^2, C^3 = c^3$$

and for $c^2 + c^3 \geq c^1$

$$C^1 = c^1, C^2 = \min\left(c^2, c^1 - \min\left(c^2, c^3, \frac{c^1}{2}\right)\right). \quad (3.30)$$

In the latter case the flow is equally distributed, if both capacities exceed the incoming flow. Otherwise, the smaller capacity is fully used and the lane with larger capacity has maximal flow under these constraints.

The numerical investigations in Section 6 show that condition 3.28 is obtained in the limit ϵ to 0 from condition (3.20) with (3.24), whereas condition 3.30 is obtained as the limit of condition 3.22 with 3.26.

3.3. Relation to coupling conditions for the ARZ equations on networks. The coupling conditions for the ARZ-equations, see [29, 35] and many others, rely on the balance of the momentum flux qz_R in the conservative formulation and the related definition of weak network solutions [32]. See the work in [23] for an exception not requiring this condition. The counterpart for the present model is the balance of the momentum flux $z = \frac{q}{1-\rho}$ which has been used here for merging junctions. However, for diverging junctions, the balance of the quantity z can in general not be prescribed anymore, if one requires that the coupling conditions lead to solutions at the nodes which remain inside the traffic domain $0 \leq \rho \leq 1$ and $0 \leq q \leq \rho$. In general, the Riemann problem is not solvable inside this domain.

We note that this is also true for the ARZ equations. In particular, the coupling conditions for the ARZ-equations in [29, 35] do not guarantee that the network solution at the nodes remain in $0 \leq \rho \leq 1$ and $0 \leq q \leq \rho$. This is easily seen by looking, for example, at the construction in [29], where values outside this region are obtained in general.

As a final remark, we note that the present model leads to much simpler explicitly solvable conditions compared to the ARZ model. This allows to investigate the coupling problem in more detail, see the asymptotic investigation as $\epsilon \rightarrow 0$ in the following sections.

4. An asymptotic procedure for the relaxation system on networks in the zero relaxation limit. In this section we relate the coupling conditions for the scalar conservation law to coupling conditions of the nonlinear relaxation system in the limit $\epsilon \rightarrow 0$. This is done via a matched asymptotic expansion using a boundary layer analysis around the node. This leads to the consideration of a half-space problem for each lane at the node. We refer to [5, 7, 18, 40] for boundary layers of kinetic equations and to [3, 38, 39, 44, 46] for investigations of boundary layers for hyperbolic relaxation systems and kinetic equations.

The general procedure is as follows: a half space layer problem is determined by a rescaling of the spatial coordinate on each lane in a spatial layer near the node. The coupling conditions for the layer problems are given by the coupling condition for the relaxation system. Finally, the asymptotic values of the layer problems are matched to half Riemann problems for the macroscopic equations. Finally, this gives the macroscopic coupling conditions for the LWR equations.

4.1. The matched asymptotic expansion on the network. We consider a single node and ingoing and outgoing lanes $[x_L^i, x_R^i]$ numbered by i . The network relaxation system is given on each lane i by the relaxation equations (2.2) for the quantities

$$\rho^i(x), q^i(x)$$

and the coupling conditions from section 3 for these values at the nodes, i.e. at $x = x_L$ or $x = x_R$ depending, whether the lane is outgoing or ingoing.

Now, the solution of the relaxation system is approximated on each lane by an asymptotic expansion. For outgoing lanes this is

$$\rho^i(x) \sim \rho_L^i\left(\frac{x - x_L}{\epsilon}\right) - \rho_L^i(\infty) + \rho_{LWR}^i(x) + \mathcal{O}(\epsilon).$$

Here $\rho_L^i(y), y \in [0, \infty)$ is the left layer solution on lane i and ρ_{LWR}^i is the LWR solution on this lane. The LWR value at the node is given by

$$\rho_{LWR}^i = \rho_{LWR}^i(x_L^i) = \rho_L^i(\infty) = \rho_K^i.$$

For ingoing lanes

$$\rho^i(x) \sim \rho_R^i\left(\frac{x_R - x}{\epsilon}\right) - \rho_R^i(\infty) + \rho_{LWR}^i(x) + \mathcal{O}(\epsilon)$$

with the layer solution $\rho_R^i(y), y \in [0, \infty)$ and

$$\rho_{LWR}^i = \rho_{LWR}^i(x_R^i) = \rho_R^i(\infty) = \rho_K^i.$$

The coupling of the asymptotic expansions at the nodes means that $\rho_L^i(0), q_L^i(0)$ for outgoing lanes and $\rho_R^i(0), q_R^i(0)$ for ingoing lanes fulfill the coupling conditions for the relaxation system, but not the characteristic equations (3.1) or (3.17).

REMARK 6. *We note that the quantities $\rho_L^i(0), q_L^i(0)$ for outgoing lanes and $\rho_R^i(0), q_R^i(0)$ for the ingoing lanes, which are denoted later on by ρ_0^i, q_0^i , are in general not equal to the values ρ^i, q^i of the solution of the relaxation system at the nodes! Both fulfill the coupling conditions, but have different characteristic equations. The transition from ρ^i, q^i to $\rho_R^i(0), q_R^i(0)$ is given through a layer in time depending on ϵ . See Figure 5.1 for a graphical discussion of the situation at the node in state space and Figure 5.2 for the corresponding time development of the solutions at the node.*

Initial conditions $(\rho_{init}^i(x), q_{init}^i(x))$ on the lanes are chosen in equilibrium, i.e. $q_{init}^i(x) = F(\rho_{init}^i(x))$ and the corresponding values at the nodes are denoted by $\rho_B^i = \rho_{init}^i(x_L)$ or $\rho_B^i = \rho_{init}^i(x_R)$ for outgoing and ingoing roads respectively. In the following we investigate first the layer equations and their asymptotic states and then the admissible half-Riemann problems for the macroscopic equations.

Showing the validity of the asymptotic procedure is then equivalent to matching the asymptotic states of the layer problems with the admissible boundary conditions for the LWR problem (i.e. half-Riemann problems for the LWR equations) and proving that there is a unique matching.

This will be done in section 5 considering the case of a merging junction with fair-merging conditions. The other cases will be treated numerically in Section 6. We proceed by discussing the layer problems.

4.2. Layer solutions for the relaxation equation. We investigate the layers of the relaxation system at the left (outgoing lanes) and the right (ingoing lanes) boundary.

4.2.1. Left layer. Consider the left boundary of the domain being located at $x = x_L$. Starting from equation (2.2) and rescaling space as $y = \frac{x-x_L}{\epsilon}$ and neglecting higher order terms in ϵ one obtains the layer equations for the left boundary for the layer solutions (ρ_L, q_L) and $y \in [0, \infty)$ as

$$\begin{aligned} \partial_y q_L &= 0 \\ \frac{q_L}{1-\rho_L} \partial_y \rho_L + \left(1 - \frac{q_L}{1-\rho_L}\right) \partial_y q_L &= -(q_L - F(\rho_L)) . \end{aligned} \quad (4.1)$$

This yields

$$\begin{aligned} q_L &= C \\ \partial_y \rho_L &= (1-\rho_L) \frac{F(\rho_L) - C}{C} . \end{aligned} \quad (4.2)$$

For $0 < C < F(\rho^*) = \sigma$, where ρ^* denotes the point where the maximum of F is attained, the above problem has two relevant fix-points

$$\rho_-(C) \leq \rho^* \quad \text{and} \quad \rho_+(C) = \tau(\rho_-) \geq \rho^* .$$

Here, $\tau(\rho) \neq \rho$ is defined by $F(\tau(\rho)) = F(\rho)$. ρ_- is instable, ρ_+ is stable. The domain of attraction of the stable fix point ρ_+ is the interval $(\rho_-, 1)$.

The third fix point $\rho = 1$ is not relevant for the further matching procedure, since it requires $C = 0$ in the macroscopic limit. In case $C = 0$ we have the instable fix point $\rho_+ = 1$ and the stable fix point $\rho_- = 0$ with domain of attraction $[0, 1)$. Moreover, we note that for $C = F(\rho^*)$ we have $\rho_- = \rho_+ = \rho^*$ and all solutions with initial values above ρ^* converge towards ρ^* , all other solutions diverge.

REMARK 7. In case of the LWR model with $F(\rho) = \rho(1-\rho)$, see Figure 4.1, we have

$$\rho_{\pm}(C) = \frac{1}{2}(1 \pm \sqrt{1-4C}) ,$$

with $C < \frac{1}{4}$. For $C = \frac{1}{4}$ we have $\rho_- = \rho_+ = \frac{1}{2}$. Moreover, $\tau(\rho) = 1 - \rho$.

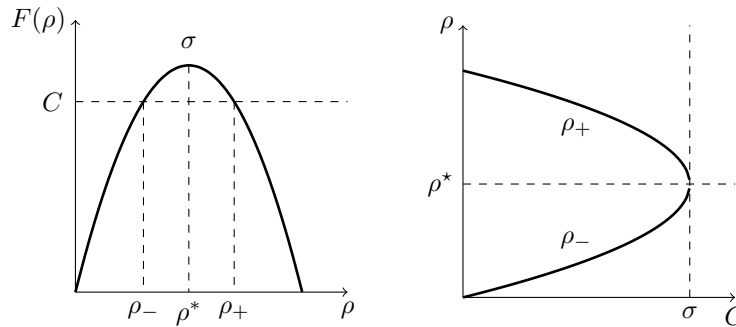


Fig. 4.1: Fundamental diagram, $F(\rho)$ and fix-points of the layer problem ρ_{\mp} .

4.2.2. Right layer. For the right boundary at x_R a scaling $y = \frac{x_R - x}{\epsilon}$ gives the layer equations for (ρ_R, q_R) and $y \in [0, \infty)$ as

$$\begin{aligned} q_R &= C \\ -\partial_y \rho_R &= (1 - \rho_R) \frac{F(\rho_R) - C}{C}. \end{aligned} \quad (4.3)$$

For $0 < C < F(\rho^*)$ the above problem has again two relevant fix points

$$\rho_-(C) \leq \rho^*, \quad \rho_+(C) = \tau(\rho_-) \geq \rho^*.$$

In this case ρ_- is stable, ρ_+ is unstable. The domain of attraction of the stable fix point ρ_- is $[0, \rho_+)$.

For $C = F(\rho^*) = \sigma$ we have $\rho_- = \rho_+ = \rho^*$ and all solutions with initial values below ρ^* converge towards ρ^* , all other solutions converge to not admissible states. For $C = 0$ we have the unstable fix point $\rho_+ = 1$ and the stable fix point $\rho_- = 0$ with domain of attraction $[0, 1)$.

4.2.3. Summary. In summary we have the following cases denoting with U the unstable fix points and with S the stable ones. Moreover, we use, as before, the notation ρ_K for the values $\rho_L(\infty)$ and $\rho_R(\infty)$ at infinity and the notation ρ_0 for the values at $y = 0$, i.e. $\rho_L(0)$ and $\rho_R(0)$.

Layer Problem at the left boundary.

$$\begin{aligned} \rho_K = \rho_-(C) &\Rightarrow \rho_0 = \rho_-(C), \quad 0 \leq C < \sigma \quad \} & (U) \\ \rho_K = \rho_+(C) &\Rightarrow \rho_0 \in (\rho_-(C), 1), \quad 0 < C < \sigma \quad \} \\ \rho_K = \rho^* &\Rightarrow \rho_0 \in [\rho^*, 1), \quad C = \sigma \quad \} & (S) \\ \rho_K = 1 &\Rightarrow \rho_0 \in (0, 1], \quad C = 0 \quad \} \end{aligned}$$

The Layer Problem at the right boundary.

$$\begin{aligned} \rho_K = \rho_+(C) &\Rightarrow \rho_0 = \rho_+(C), \quad 0 \leq C < \sigma \quad \} & (U) \\ \rho_K = \rho_-(C) &\Rightarrow \rho_0 \in [0, \rho_+(C)), \quad 0 < C < \sigma \quad \} \\ \rho_K = \rho^* &\Rightarrow \rho_0 \in [0, \rho^*], \quad C = \sigma \quad \} & (S) \\ \rho_K = 0 &\Rightarrow \rho_0 \in [0, 1), \quad C = 0 \quad \} \end{aligned}$$

We use for the three cases of the stable fix point (S) the notation

$$\rho_K = \rho_+(C) \quad \Rightarrow \quad \rho(0) \in [\rho_-(C), 1], 0 \leq C \leq \sigma$$

for the left boundary and

$$\rho_K = \rho_-(C) \quad \Rightarrow \quad \rho(0) \in [0, \rho_+(C)], 0 \leq C \leq \sigma$$

for the right boundary.

4.3. Half-Riemann problems for the limit conservation law. We consider the limit conservation law $\partial_t \rho + \partial_x F(\rho) = 0$. The initial trace at the boundary of the scalar equation is as before denoted by ρ_B . For a matching of layer solutions and solutions of the scalar conservation, those states ρ_K are required which can be connected to ρ_B with LWR-waves (shocks and rarefaction waves) with non-negative velocity at the left and non-positive velocity at the right boundary. They are summarized in the following:

The half-Riemann problem at the left boundary.

$$\begin{aligned}\rho_B \leq \rho^* \text{ (RP 1)} & \Rightarrow \rho_K \in [0, \rho^*] \\ \rho_B > \rho^* \text{ (RP 2)} & \Rightarrow \rho_K \in [0, \tau(\rho_B)] \cup \{\rho_B\}\end{aligned}$$

The half-Riemann problem at the right boundary.

$$\begin{aligned}\rho_B \geq \rho^* \text{ (RP 1)} & \Rightarrow \rho_K \in [\rho^*, 1] \\ \rho_B < \rho^* \text{ (RP 2)} & \Rightarrow \rho_K \in \{\rho_B\} \cup [\tau(\rho_B), 1]\end{aligned}$$

5. The asymptotic procedure for merging junctions. Here we consider the merging case with coupling conditions (3.6), i.e. the equality of densities, in detail. First we investigate the layers of the relaxation system at the nodes coupled to each other via the coupling conditions and determine resulting conditions on their asymptotic states. Then, we match these results to Riemann solutions of the macroscopic problems on each of the roads. The main result of this section is to show, that the asymptotic procedure starting from the relaxation network with the conditions (3.6) leads in the limit $\epsilon \rightarrow 0$ to the LWR-network with the fair merging conditions 3.15.

Assuming the boundary traces $\rho_B^i, i = 1, 2, 3$ on the three roads to be given, we have to determine the new states ρ_K^i at the node. On the one hand ρ_K^i are the asymptotic states of the respective layer problems, on the other hand they are the right (for road 1 and 2) or left (for road 3) states of the half-Riemann problems for the LWR equations, i.e. the boundary conditions for the LWR equations. The states at the junction in the asymptotic limit (corresponding to $y = 0$ for the layers) are denoted in the following by ρ_0^i and determined together with the other values. We have to consider eight different configurations of Riemann problems. For each of them all possible combinations with stable or unstable layer solutions have to be discussed. Not admissible combinations are not listed. We give first a detailed discussion of the coupling of the layer solutions in section 5.1 and second a discussion of the matching of the layer solutions to the half Riemann problems on the respective roads in section 5.2.

REMARK 8. A similar procedure could be used for the other conditions. We limit ourselves to a numerical investigation, see Section 6.

5.1. Coupling the layers. Here, we consider the coupling of the layers at the node. The states at the junction (corresponding to the ingoing states at $y = 0$ for the layers) are ρ_0^i . Each layer can have either a stable solution (S) or an unstable solution (U). Thus, for three lanes we have eight possible combinations, which be denote by U/S-U/S-U/S.

Case1, U-U-U. We have $\rho_0^1 = \rho_+(C^1), \rho_0^2 = \rho_+(C^2), \rho_0^3 = \rho_-(C^3)$, compare subsection 4.2.3. The coupling conditions give

$$\begin{aligned}\rho_+(C^1) = \rho_+(C^2) = \rho_-(C^3) \\ C^3 = C^1 + C^2\end{aligned}$$

with $0 \leq C^1, C^2, C^3 < \sigma$.

The second equality gives $C^2 = C^3 = \sigma$. This is not consistent with the range of C^2 and C^3 . The case is not admissible.

Case 2, S-U-U According to subsection 4.2.3, we have $\rho_0^1 \in [0, \rho_+(C^1)]$ and $\rho_0^2 = \rho_+(C^2), \rho_0^3 = \rho_-(C^3)$. Inserting into the coupling conditions gives

$$\begin{aligned}\rho_0^1 = \rho_+(C^2) = \rho_-(C^3) \\ C^3 = C^1 + C^2\end{aligned}$$

with $0 \leq C^1 \leq \sigma$ and $0 \leq C^2, C^3 < \sigma$. Again the second equation gives $C^2 = C^3 = \sigma$ which is not in the range of C^2, C^3 . The case is not admissible.

Case 3, U-S-U We have $\rho_0^1 = \rho_+(C^1), \rho_0^2 \in [0, \rho_+(C^2)], \rho_0^3 = \rho_-(C^3)$. The case is symmetric to the above and not admissible.

Case 4, U-U-S We have $\rho_0^1 = \rho_+(C^1), \rho_0^2 = \rho_+(C^2), \rho_0^3 = [\rho_-(C^3), 1]$. We have

$$\begin{aligned}\rho_+(C^1) &= \rho_+(C^2) = \rho_0^3 \\ C^3 &= C^1 + C^2\end{aligned}$$

with $0 \leq C^1, C^2 < \sigma$ and $0 \leq C^3 \leq \sigma$. This gives $C^1 = C^2 = \frac{C^3}{2}$ and

$$\rho_0^1 = \rho_0^2 = \rho_0^3 = \rho_+\left(\frac{C^3}{2}\right).$$

Case 5, U-S-S We have $\rho_0^1 = \rho_+(C^1), \rho_0^2 \in [0, \rho_+(C^2)]$ and $\rho_0^3 \in [\rho_-(C^3), 1]$ with $0 \leq C^1 < \sigma$ and $0 \leq C^2, C^3 \leq \sigma$. We have

$$\begin{aligned}\rho_+(C^1) &= \rho_0^2 = \rho_0^3 \\ C^3 &= C^1 + C^2.\end{aligned}$$

This gives $\rho_0^2 = \rho_0^3 = \rho_+(C^1) = \rho_+(C^3 - C^2)$ with the requirement $0 \leq C^3 - C^2 \leq \sigma$ or $C^3 \geq C^2$ and $\rho_0^2 = \rho_0^3 = \rho_+(C^3 - C^2) \in [\rho_-(C^3), \rho_+(C^2)]$. It leads to $\rho_+(C^3 - C^2) \leq \rho_+(C^2)$ or $C^3 - C^2 \geq C^2$ or $C^3 \geq 2C^2$. Altogether, we have for $2C^2 \leq C^3$ and $C^1 = C^3 - C^2$

$$\rho_0^1 = \rho_0^2 = \rho_0^3 = \rho_+(C^3 - C^2).$$

Case 6, S-U-S We have $\rho_0^1 \in [0, \rho_+(C^1)]$ and $\rho_0^2 = \rho_+(C^2), \rho_0^3 \in [\rho_-(C^3), 1]$ with $0 \leq C^1 \leq \sigma$ and $0 \leq C^2, C^3 < \sigma$. The case is symmetric to case 5. For $2C^1 \leq C^3$ and $C^2 = C^3 - C^1$ we have

$$\rho_0^1 = \rho_0^2 = \rho_0^3 = \rho_+(C^3 - C^1).$$

Case 7, S-S-U We have $\rho_0^1 \in [0, \rho_+(C^1)]$ and $\rho_0^2 \in [0, \rho_+(C^2)]$ and $\rho_0^3 = \rho_-(C^3)$ with $0 \leq C^1, C^2 \leq \sigma$ and $0 \leq C^3 < \sigma$. The coupling conditions give

$$\begin{aligned}\rho_0^1 &= \rho_0^2 = \rho_-(C^3) \\ C^3 &= C^1 + C^2.\end{aligned}$$

This gives $\rho_0^1 = \rho_0^2 = \rho_-(C^3)$ with the condition $0 \leq C^1 + C^2 < \sigma$. Thus, for $0 \leq C^1 + C^2 < \sigma$ we have

$$\rho_0^1 = \rho_0^2 = \rho_0^3 = \rho_-(C^1 + C^2).$$

Case 8, S-S-S We have $\rho_0^1 \in [0, \rho_+(C^1)], \rho_0^2 \in [0, \rho_+(C^2)], \rho_0^3 \in [\rho_-(C^3), 1]$ with $0 \leq C^1, C^2, C^3 \leq \sigma$. The conditions are

$$\begin{aligned}\rho_0^1 &= \rho_0^2 = \rho_0^3 \\ C^3 &= C^1 + C^2.\end{aligned}$$

The values of $\rho_0^1 = \rho_0^2 = \rho_0^3$ are not uniquely determined, but they are restricted to the interval $[\rho_-(C^1 + C^2), \min(\rho_+(C^1), \rho_+(C^2))]$.

These considerations yield all possible combinations of layer problems at the node. Now, they have to be matched to the half-Riemann problems at the respective lanes.

5.2. Matching of Riemann problem and layer equations. Assuming the initial states $\rho_B^i, i = 1, 2, 3$ to be given, we have to determine the fluxes C^i and new states ρ_K^i at the node. As mentioned, on the one hand ρ_K^i are the asymptotic states of the respective layer problems fulfilling the conditions in the last section 5.1. On the other hand they are the left (road 1 and 2) or right (road 3) states of the half Riemann problems which have to be connected with ρ_B^i . As before, ρ_0^i are the states at the junction in the limit $\epsilon \rightarrow 0$.

We consider eight different configurations for the states ρ_B^i corresponding to the possible combinations of different half Riemann problems. For each of them all possible combinations with stable or unstable layer solutions have to be discussed. Not admissible combinations are not listed. We consider the cases ordered in terms of the different possible combinations of Riemann problems on the 3 roads using the notation RP1/2-1/2-1/2 for the respective combination of the half Riemann problems.

Case 1, RP1-1-1 $\rho_B^1 \geq \rho^*, \rho_B^2 \geq \rho^*, \rho_B^3 \leq \rho^*$. From Section 4.3 we obtain

$$\begin{aligned} \rho_K^1 \in [\rho^*, 1] : & \quad (U) \text{ or } ((S) \text{ with } C^1 = \sigma) \\ \rho_K^2 \in [\rho^*, 1] : & \quad (U) \text{ or } ((S) \text{ with } C^2 = \sigma) \\ \rho_K^3 \in [0, \rho^*] : & \quad (U) \text{ or } ((S) \text{ with } C^3 = \sigma) \end{aligned}$$

Then, the discussion in Section 5.1 leads to 5 different cases:

UUS with $C^3 = \sigma$ and $C^1 = C^2 = \frac{\sigma}{2}$ and $\rho_0^3 = \rho_+(\frac{\sigma}{2})$.

USS with $C^2 = C^3 = \sigma$ which contradicts $C^3 \geq 2C^2$.

SUS with $C^1 = C^3 = \sigma$ which contradicts $C^3 \geq 2C^1$.

SSU with $C^1 = C^2 = \sigma$ and a contradiction to $C^1 + C^2 \leq \sigma$.

SSS with $C^1 = C^2 = C^3 = \sigma$, which gives a contradiction to the balance of fluxes. This gives $C_1 = C_2 = \frac{\sigma}{2}, C_3 = \sigma$ and $\rho_0^i = \rho_+(\frac{\sigma}{2})$. The values for ρ_K^i follow directly.

Case 2, RP1-1-2 $\rho_B^1 \geq \rho^*, \rho_B^2 \geq \rho^*, \rho_B^3 \geq \rho^*$.

$$\begin{aligned} \rho_K^1 \in [\rho^*, 1] : & \quad (U) \text{ or } ((S) \text{ with } C^1 = \sigma) \\ \rho_K^2 \in [\rho^*, 1] : & \quad (U) \text{ or } ((S) \text{ with } C^2 = \sigma) \\ \rho_K^3 \in [0, \tau(\rho_B^3)] \cup \{\rho_B^3\} : & \quad ((U) \text{ with } C^3 \leq F(\rho_B^3)) \text{ or } ((S) \text{ with } C^3 = F(\rho_B^3)) \end{aligned}$$

UUS with $C^3 = F(\rho_B^3)$ and $C^1 = C^2 = \frac{1}{2}F(\rho_B^3)$ and $\rho_0^3 = \rho_+(\frac{1}{2}F(\rho_B^3))$.

USS with $C^2 = \sigma$ which contradicts $C^3 \geq 2C^2$.

SUS with $C^1 = \sigma$ which contradicts $C^3 \geq 2C^1$.

SSU with $C^1 = C^2 = \sigma$ and a contradiction to $C^1 + C^2 \leq \sigma$.

SSS with $C^1 = C^2 = C^3 = \sigma$, which gives a contradiction to the balance of fluxes. This gives $C_1 = C_2 = F(\frac{\rho_B^3}{2}), C_3 = F(\rho_B^3)$ and $\rho_0^i = \rho_+(\frac{1}{2}F(\rho_B^3))$.

Case 3, RP1-2-1 $\rho_B^1 \geq \rho^*, \rho_B^2 \leq \rho^*, \rho_B^3 \leq \rho^*$.

$$\begin{aligned} \rho_K^1 \in [\rho^*, 1] : & \quad (U) \text{ or } ((S) \text{ with } C^1 = \sigma) \\ \rho_K^2 \in [\tau(\rho_B^2), 1] \cup \{\rho_B^2\} : & \quad ((U) \text{ with } C^2 \leq F(\rho_B^2)) \text{ or } ((S) \text{ with } C^2 = F(\rho_B^2)) \\ \rho_K^3 \in [\rho^*, 1] : & \quad (U) \text{ or } ((S) \text{ with } C^3 = \sigma) \end{aligned}$$

UUS with $C^3 = \sigma$ which gives $C^1 = C^2 = \frac{\sigma}{2}$. Moreover, $C^2 \leq F(\rho_B^2)$. This is possible, if $\frac{\sigma}{2} \leq F(\rho_B^2)$. Then, $\rho_0^3 = \rho_+(\frac{\sigma}{2})$

USS with $C^3 = \sigma, C^2 = F(\rho_B^2)$. $C^3 \geq 2C^2$ gives the requirement $\frac{\sigma}{2} \geq F(\rho_B^2)$.
Moreover, we have $C^1 = \sigma - F(\rho_B^2)$ and $\rho_0^2 = \rho_0^3 = \rho_+(C^1)$.

SUS with $C^1 = \sigma$ which contradicts $C^3 \geq 2C^1$.

SSU with $C^1 = \sigma$ and $C^2 = F(\rho_B^2)$. This is only possible for $\rho_B^2 = 0$ and $C^2 = 0$.
Then $C^3 = \sigma$ and $\rho_0^i = \rho_-(\sigma) = \rho^*$.

SSS with $C^1 = C^3 = \sigma$ and $C^2 = F(\rho_B^2)$. This gives again $\rho_B^2 = 0$ and $C^2 = 0$.
Then $\rho_0^i \in [\rho_-(C^1 + C^2), \min(\rho_+(C^1), \rho_+(C^2))]$ gives $\rho_0^i \in [\rho_-(\sigma), \rho_+(\sigma)]$.
This leaves only $\rho_0^i = \rho^*$.

This gives for $\frac{\sigma}{2} \leq F(\rho_B^2)$ that $C^1 = C^2 = \frac{C^3}{2} = \frac{\sigma}{2}$ and $\rho_0^i = \rho_+(\frac{\sigma}{2})$.

For $\frac{\sigma}{2} \geq F(\rho_B^2)$ one has $C^1 = \sigma - F(\rho_B^2)$, $C^3 = \sigma, C^2 = F(\rho_B^2)$ and $\rho_0^i = \rho_+(\sigma - F(\rho_B^2))$.

Case 4, RP2-1-1 $\rho_B^1 \leq \rho^*, \rho_B^2 \geq \rho^*, \rho_B^3 \leq \rho^*$. This case is symmetric to Case 3.

We have for $\frac{\sigma}{2} \geq F(\rho_B^1)$ that $C^1 = F(\rho_B^1), C^3 = \sigma$, $C^2 = \sigma - F(\rho_B^1)$ and $\rho_0^i = \rho_+(\sigma - F(\rho_B^1))$.

For $\frac{\sigma}{2} \leq F(\rho_B^1)$ one has $C^1 = C^2 = \frac{C^3}{2} = \frac{\sigma}{2}$ and $\rho_0^i = \rho_+(\frac{\sigma}{2})$.

Case 5, RP1-2-2 $\rho_B^1 \geq \rho^*, \rho_B^2 \leq \rho^*, \rho_B^3 \geq \rho^*$.

$$\begin{aligned} \rho_K^1 &\in [\rho^*, 1] : && (U) \text{ or } ((S) \text{ with } C^1 = \sigma) \\ \rho_K^2 &\in [\tau(\rho_B^2), 1] \cup \{\rho_B^2\} : && ((U) \text{ with } C^2 \leq F(\rho_B^2)) \text{ or } ((S) \text{ with } C^2 = F(\rho_B^2)) \\ \rho_K^3 &\in [0, 1 - \rho_B^3] \cup \{\rho_B^3\} : && ((U) \text{ with } C^3 \leq F(\rho_B^3)) \text{ or } ((S) \text{ with } C^3 = F(\rho_B^3)) \end{aligned}$$

UUS with $C^2 \leq F(\rho_B^2)$ and $C^3 = F(\rho_B^3)$. If $F(\rho_B^3) \leq 2F(\rho_B^2)$ then $C^1 = C^2 = \frac{F(\rho_B^3)}{2}$ and $\rho_0^3 = \rho_+(\frac{C^3}{2})$.

USS with $C^2 = F(\rho_B^2), C^3 = F(\rho_B^3)$. With $C^3 \geq 2C^2$ or $F(\rho_B^3) \geq F(\rho_B^2)$ we have $C^1 = C^3 - C^2$.

SUS with $C^1 = \sigma, C^2 \leq F(\rho_B^2), C^3 = F(\rho_B^3)$, which gives a contradiction to $C^3 \geq 2C^1$.

SSU with $C^1 = \sigma$ and $C^2 = F(\rho_B^2), C^3 \leq F(\rho_B^3)$. This is only possible for $\rho_B^2 = 0$.
Then $C^3 = \sigma, \rho_B^3 = \rho^*$ and $\rho_0^i = \rho_-(\sigma) = \rho^*$.

SSS with $C^1 = \sigma$ and $C^2 = F(\rho_B^2), C^3 = F(\rho_B^3)$. This is only possible, if $C^2 = 0$ and $\rho_B^2 = 0$. This yields $C^3 = \sigma$ and $\rho_B^3 = \rho^*$. Then $\rho_0^i \in [\rho_-(C^1 + C^2), \min(\rho_+(C^1), \rho_+(C^2))]$ gives $\rho_0^i \in [\rho_-(\sigma), \rho_+(\sigma)]$, which leaves only $\rho_0^i = \rho^*$.

This gives for $F(\rho_B^3) \leq 2F(\rho_B^2)$ that $C_1 = \frac{F(\rho_B^3)}{2} = C_2, C_3 = F(\rho_B^3)$ and $\rho_0^i = \rho_+(\frac{F(\rho_B^3)}{2})$.

For $F(\rho_B^3) \geq 2F(\rho_B^2)$ one has $C_1 = F(\rho_B^3) - F(\rho_B^2), C_2 = F(\rho_B^2), C_3 = F(\rho_B^3)$ and $\rho_0^i = \rho_+(F(\rho_B^3) - F(\rho_B^2))$.

Case 6, RP2-1-2 $\rho_B^1 \leq \rho^*, \rho_B^2 \geq \rho^*, \rho_B^3 \geq \rho^*$. This case is symmetric to case 5.

We have for $F(\rho_B^3) \leq 2F(\rho_B^1)$ that $C_1 = \frac{F(\rho_B^3)}{2} = C_2, C_3 = F(\rho_B^3)$ and $\rho_0^i = \rho_+(\frac{F(\rho_B^3)}{2})$.

For $F(\rho_B^3) \geq 2F(\rho_B^1)$ one has $C_1 = F(\rho_B^1), C_2 = F(\rho_B^3) - F(\rho_B^1), C_3 = F(\rho_B^3)$ and $\rho_0^i = \rho_+(F(\rho_B^3) - F(\rho_B^1))$.

Case 7, RP2-2-1 $\rho_B^1 \leq \rho^*, \rho_B^2 \leq \rho^*, \rho_B^3 \leq \rho^*$.

$$\begin{aligned} \rho_K^1 &\in [\tau(\rho_B^1), 1] \cup \{\rho_B^1\} : && ((U) \text{ with } C^1 \leq F(\rho_B^1)) \text{ or } ((S) \text{ with } C^1 = F(\rho_B^1)) \\ \rho_K^2 &\in [\tau(\rho_B^2), 1] \cup \{\rho_B^2\} : && ((U) \text{ with } C^2 \leq F(\rho_B^2)) \text{ or } ((S) \text{ with } C^2 = F(\rho_B^2)) \\ \rho_K^3 &\in [0, \rho^*] : && (U) \text{ or } ((S) \text{ with } C^3 = \sigma) \end{aligned}$$

UUS with $C^1 \leq F(\rho_B^1)$ and $C^2 \leq F(\rho_B^2)$. $C^3 = \sigma$ yields $C^1 = C^2 = \frac{\sigma}{2}$, if $F(\rho_B^1) \geq \frac{\sigma}{2}$ and $F(\rho_B^2) \geq \frac{\sigma}{2}$. Then $\rho_0^3 = \rho_+(\frac{C^3}{2})$.

USS with $C^1 \leq F(\rho_B^1)$, $C^3 = \sigma$, $C^2 = F(\rho_B^2)$. $C^3 \geq 2C^2$ is equivalent to $\frac{\sigma}{2} \geq F(\rho_B^2)$. Moreover, $C^1 = \sigma - F(\rho_B^2)$ requires $F(\rho_B^1) + F(\rho_B^2) \geq \sigma$.

SUS with $C^1 = F(\rho_B^1)$, $C^2 \leq F(\rho_B^2)$, $C^3 = \sigma$. $C^3 \geq 2C^1$ gives $\frac{\sigma}{2} \geq F(\rho_B^1)$, $F(\rho_B^2) \geq \frac{\sigma}{2}$ and $C^2 = \sigma - F(\rho_B^1) \geq \frac{\sigma}{2}$. Moreover, $\rho_0^1 = \rho_+(C^3 - C^1)$.

SSU with $C^1 = F(\rho_B^1)$ and $C^2 = F(\rho_B^2)$. This gives $F(\rho_B^1) + F(\rho_B^2) \leq \sigma$ and $\rho_0^i = \rho_-(C^3)$.

SSS with $C^1 = F(\rho_B^1)$ and $C^2 = F(\rho_B^2)$, $C^3 = \sigma$. This is only possible, if $F(\rho_B^1) + F(\rho_B^2) = \sigma$. In this case, since $\rho_0^i \in [\rho_-(C^1 + C^2), \min(\rho_+(C^1), \rho_+(C^2))]$ we obtain $\rho_0^i \in [\rho_-(\sigma), \min(\rho_+(F(\rho_B^1)), \rho_+(F(\rho_B^2)))]$. This gives the restriction $\rho_0^i \in [\rho^*, \min(\tau(\rho_B^1), \tau(\rho_B^2))]$ according to the range of ρ_B^1, ρ_B^2 .

We obtain for $F(\rho_B^1) + F(\rho_B^2) \leq \sigma$ (**SSU**) that $C_1 = F(\rho_B^1)$, $C_2 = F(\rho_B^2)$, $C_3 = F(\rho_B^1) + F(\rho_B^2)$ and $\rho_0^i = \rho_-(F(\rho_B^1) + F(\rho_B^2))$.

For $F(\rho_B^1) + F(\rho_B^2) \geq \sigma$, $F(\rho_B^1) \geq \frac{\sigma}{2}$, $F(\rho_B^2) \geq \frac{\sigma}{2}$ (**UUS**) one has $C_1 = \frac{\sigma}{2} = C^2$, $C^3 = \sigma$ and $\rho_0^i = \rho_+(\frac{\sigma}{2})$.

For $F(\rho_B^1) + F(\rho_B^2) \geq \sigma$, $F(\rho_B^1) \leq \frac{\sigma}{2}$, $F(\rho_B^2) \geq \frac{\sigma}{2}$ (**SUS**) one has $C_1 = F(\rho_B^1)$, $C_2 = \sigma - F(\rho_B^1)$, $C_3 = \sigma$ and $\rho_0^i = \rho_+(\sigma - F(\rho_B^1))$.

For $F(\rho_B^1) + F(\rho_B^2) \geq \sigma$, $F(\rho_B^1) \geq \frac{\sigma}{2}$, $F(\rho_B^2) \leq \frac{\sigma}{2}$ (**USS**) one has $C_1 = \sigma - F(\rho_B^2)$, $C_2 = F(\rho_B^2)$, $C_3 = \sigma$ and $\rho_0^i = \rho_+(\sigma - F(\rho_B^2))$.

REMARK 9. We note that at the interfaces between the different conditions we obtain values $\rho_0^i \in [\rho^*, \min(\rho_+(F(\rho_B^1)), \rho_+(F(\rho_B^2)))]$. This is exactly the interval for the ρ^i -values in case (**SSS**).

Case 8, RP2-2-2 $\rho_B^1 \leq \rho^*, \rho_B^2 \leq \rho^*, \rho_B^3 \geq \rho^*$.

$$\begin{aligned} \rho_K^1 &\in [\tau(\rho_B^1), 1] \cup \{\rho_B^1\} : && ((U) \text{ with } C^1 \leq F(\rho_B^1)) \text{ or } ((S) \text{ with } C^1 = F(\rho_B^1)) \\ \rho_K^2 &\in [\tau(\rho_B^2), 1] \cup \{\rho_B^2\} : && ((U) \text{ with } C^2 \leq F(\rho_B^2)) \text{ or } ((S) \text{ with } C^2 = F(\rho_B^2)) \\ \rho_K^3 &\in [0, \tau(\rho_B^3)] \cup \{\rho_B^3\} : && ((U) \text{ with } C^3 \leq F(\rho_B^3)) \text{ or } ((S) \text{ with } C^3 = F(\rho_B^3)) \end{aligned}$$

UUS with $C^1 \leq F(\rho_B^1)$, $C^2 \leq F(\rho_B^2)$ and $C^3 = F(\rho_B^3)$. If $F(\rho_B^3) \leq 2F(\rho_B^1)$ and $F(\rho_B^3) \leq 2F(\rho_B^2)$ then $C^1 = C^2 = \frac{F(\rho_B^3)}{2}$ and $\rho_0^3 = \rho_+(\frac{C^3}{2})$.

USS with $C^1 \leq F(\rho_B^1)$, $C^2 = F(\rho_B^2)$, $C^3 = F(\rho_B^3)$. With $C^3 \geq 2C^2$ we have $F(\rho_B^3) \geq 2F(\rho_B^2)$ and $F(\rho_B^3) - F(\rho_B^2) \leq F(\rho_B^1)$ or $F(\rho_B^1) + F(\rho_B^2) \geq F(\rho_B^3)$.

SUS with $C^1 = F(\rho_B^1)$, $C^2 \leq F(\rho_B^2)$, $C^3 = F(\rho_B^3)$. $C^3 \geq 2C^1$ gives $F(\rho_B^3) \geq 2F(\rho_B^1)$ and $F(\rho_B^3) - F(\rho_B^1) \leq F(\rho_B^2)$ or $F(\rho_B^1) + F(\rho_B^2) \geq F(\rho_B^3)$. Moreover $\rho_0^1 = \rho_+(C^3 - C^1)$.

SSU with $C^1 = F(\rho_B^1)$ and $C^2 = F(\rho_B^2)$, $C^3 \leq F(\rho_B^3)$. This is only possible for $F(\rho_B^1) + F(\rho_B^2) \leq F(\rho_B^3)$. Moreover, $\rho_0^i = \rho_-(C^3)$.

SSS with $C^1 = F(\rho_B^1)$ and $C^2 = F(\rho_B^2)$, $C^3 = F(\rho_B^3)$. This is only possible, if $F(\rho_B^1) + F(\rho_B^2) = F(\rho_B^3)$.

We obtain $\rho_0^i \in [\rho_-(F(\rho_B^3)), \min(\rho_+(F(\rho_B^1)), \rho_+(F(\rho_B^2)))]$. This gives according to the range of ρ_B^2, ρ_B^3 , that $\rho_0^i \in [\tau(\rho_B^3), \min(\tau(\rho_B^1), \tau(\rho_B^2))]$.

This gives for $F(\rho_B^3) \leq 2F(\rho_B^1)$ and $F(\rho_B^3) \leq 2F(\rho_B^2)$ (*UUS*) that $C_1 = \frac{F(\rho_B^3)}{2} = C^2, C_3 = F(\rho_B^3)$ and $\rho_0^i = \rho_+(\frac{F(\rho_B^3)}{2})$.

For $F(\rho_B^3) \geq 2F(\rho_B^2)$ and $F(\rho_B^1) + F(\rho_B^2) \geq F(\rho_B^3)$ (*USS*) one has $C^2 = F(\rho_B^2), C^3 = F(\rho_B^3), C_1 = F(\rho_B^3) - F(\rho_B^2)$ and $\rho_0^i = \rho_+(F(\rho_B^3) - F(\rho_B^2))$.

For $F(\rho_B^3) \geq 2F(\rho_B^1)$ and $F(\rho_B^1) + F(\rho_B^2) \geq F(\rho_B^3)$ (*SUS*) one has $C_1 = F(\rho_B^1), C^3 = F(\rho_B^3), C^2 = F(\rho_B^3) - F(\rho_B^1)$ and $\rho_0^i = \rho_+(F(\rho_B^3) - F(\rho_B^1))$.

For $F(\rho_B^1) + F(\rho_B^2) \leq F(\rho_B^3)$ (*SSU*) one has $C_1 = F(\rho_B^1), C^2 = F(\rho_B^2), C^3 = F(\rho_B^1) + F(\rho_B^2)$ and $\rho_0^i = \rho_-(F(\rho_B^1) + F(\rho_B^2))$.

REMARK 10. Note that the sub-cases in Case 8 partition uniquely the range of admissible states since for $0 \leq x, y, z \leq 1$ either $(x + y \leq z)$ or $(x + y \geq z$ and $z \geq 2y)$ or $(x + y \geq z$ and $z \geq 2x)$ or $(z \leq 2x$ and $z \leq 2y)$. Moreover, note that at the interfaces between the different conditions we obtain that $\rho_0^i \in [\rho_-(F(\rho_B^3)), \min(\rho_+(F(\rho_B^1)), \rho_+(F(\rho_B^2)))]$. This is exactly the interval for the ρ^i -values in case (*SSS*).

The above computations show that there is a unique matching of layer solutions and LWR solutions and that the asymptotic expansion lead to well defined conditions for the LWR network.

Considering only the fluxes and neglecting the information on the ρ_0^i the above result can be rewritten in a more convenient way using the supply- and demand formulation, see section 3.1.2 or [36]. We obtain

Case 1, RP1-1-1. This is a case with $c^1, c^2 \leq \frac{c^3}{2} : C^1 = c^1, C^2 = c^2$.

Case 2, RP1-1-2. This is a case with $c^1, c^2 \geq \frac{c^3}{2} : C^1 = C^2 = \frac{c^3}{2}$.

Case 3, RP1-2-1 We have $c^1 \geq c^2$ and two cases:

$$c^2 \geq \frac{c^3}{2} : C^1 = C^2 = \frac{c^3}{2}$$

$$c^2 \leq \frac{c^3}{2} : C^1 = c^3 - c^2, C^2 = c^2.$$

Case 4, RP2-1-1 Symmetric to Case 3. We have $c^1 \leq c^2$ and two cases:

$$c^1 \geq \frac{c^3}{2} : C^1 = C^2 = \frac{c^3}{2}$$

$$c^1 \leq \frac{c^3}{2} : C^1 = c^1, C^2 = c^3 - c^1.$$

Case 5, RP1-2-2 In terms of the c^i this case is the same as Case 3.

Case 6, RP2-1-2 This case is the same as Case 4.

Case 7, RP2-2-1 We have four cases:

$$c^1 + c^2 \leq c^3 : C^1 = c^1, C^2 = c^2$$

$$c^1 + c^2 \geq c^3, c^1 \geq \frac{c^3}{2}, c^2 \geq \frac{c^3}{2} : C^1 = C^2 = \frac{c^3}{2}$$

$$c^1 + c^2 \geq c^3, c^1 \geq \frac{c^3}{2}, c^2 \leq \frac{c^3}{2} : C^1 = c^3 - c^2, C^2 = c^2$$

$$c^1 + c^2 \geq c^3, c^1 \leq \frac{c^3}{2}, c^2 \geq \frac{c^3}{2} : C^1 = c^1, C^2 = c^3 - c^1.$$

Case 8, RP2-2-2 We obtain the same as in Case 7.

One observes directly, that this result can be rewritten in the more compact form given in 3.15 which shows that the relaxation network with conditions (3.6) converges for $\epsilon \rightarrow 0$ to the LWR network with the fair merging conditions (3.15).

REMARK 11. *The above derivation shows that the classical merge condition (3.15) for the LWR-network can be obtained as the asymptotic limit of condition (3.6) for the relaxation system, that means the equality of densities. The equality of densities is not fulfilled on the macroscopic level of the conservation law, only the balance of fluxes is common for both levels of coupling conditions. Moreover, we note that this is not the only coupling condition for the relaxation system leading to (3.15). A similar investigation leading to the same macroscopic coupling conditions could be performed for condition (3.11), i.e. the priority condition with priority $P = \frac{1}{2}$.*

A graphical sketch of the different quantities in state space is given in Figure 5.1 for the special example $\rho_B^1 = 0.2$, $\rho_B^2 = 0.3$ and $\rho_B^3 = 0.6$. One observes the difference at the junction between the values $\bar{\rho} = \rho^i$ found by solving the coupling conditions for the relaxation system and the values $\bar{\rho}_0 = \rho_0^i$ found by the asymptotic investigation. We note that both values fulfill the coupling conditions, but different equations (characteristic equations for the relaxation system versus layer plus LWR-wave for the limit problem) connecting them to the ρ_B^i . The time development of the value at the nodes for the relaxation system with different ϵ is shown in Figure 5.2. One observes the evolution of the values at the junction from $\bar{\rho}$ to $\bar{\rho}_0$. The size of the temporal layer in Figure 5.2 also depends on ϵ .

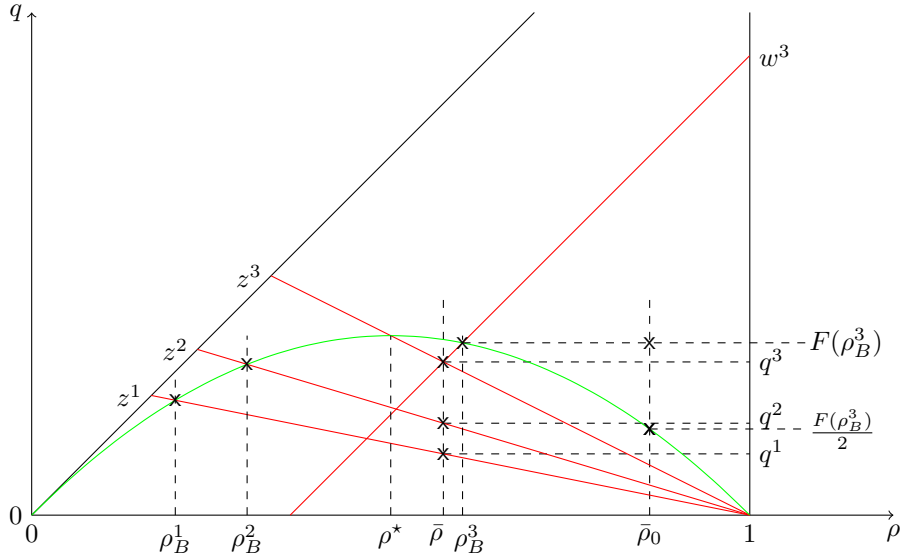


Fig. 5.1: Fair merging coupling conditions with $\rho_B^1 = 0.2$, $\rho_B^2 = 0.3$ and $\rho_B^3 = 0.6$. $\bar{\rho}$ is the value found from solving (3.6) at the node and $\bar{\rho}_0$ is the ingoing value of the solution of the layer problems at the node found from the analysis in Section 5.2.

6. Numerical results. In this section we compare relaxation and macroscopic network solutions with the different coupling conditions for several characteristic numerical examples. The relaxation model is discretized in its conservative form (2.3) using a Godunov scheme. A Godunov scheme is also used for the LWR model. In all

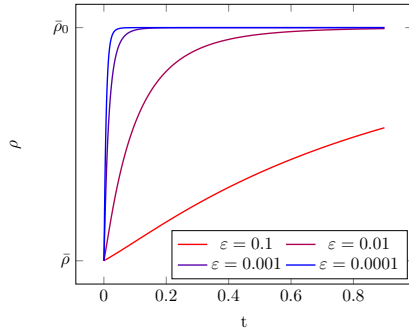


Fig. 5.2: Solution of the relaxation system with different values of ε for the initial values in Figure 5.1. Time development of the density at the junction from $\bar{\rho}$ to $\bar{\rho}_0$.

numerical examples the intervals on the edges $[0, 1]$ are discretized with 1000 cell. The ingoing edges are connected to the junction at $x = 1$, while the cars enter at $x = 0$ into the outgoing edges. At the outer boundaries zero-Neumann boundary conditions are imposed. The scaling parameter ε in the relaxation system is chosen as $\varepsilon = 0.001$. As initial conditions the densities ρ^i are chosen constant on each road. The additional initial condition for z^i in the relaxation model is chosen in equilibrium $z^i = \frac{F(\rho^i)}{1-\rho^i}$. All solutions are computed up to $T = 1$.

6.1. Fair merging. First we compare the numerical solutions of the relaxation model with the coupling conditions 3.6 with the results obtained for the LWR model with the coupling conditions (3.15). In Figure 6.1 the initial densities are chosen as $\rho^1 = 0.1$, $\rho^2 = 0.15$ and $\rho^3 = 0.2$. The densities are small enough, such that all cars can pass the junction, which corresponds to Case 7, first subcase. The ρ_0^i are given by $\rho_-(F(\rho_B^1) + F(\rho_B^2))$ with the numerical value $\rho_0^i = 0.3197$. In Figure 6.1 the numerical solutions are shown. Outside of the layer regions, the solution of the relaxation model (blue) is almost identical to the solution of the LWR model (red). In the second row a zoom into the layer regions at the junctions is shown. On edge 1 and 2 we can observe two boundary layers, as these correspond to stable cases. In edge 3 there is no layer, since the half space solution is unstable. The solution at $x = 0$ fits exactly to the analytical value of ρ_0^i .

In Figure 6.2 the numerical solutions to the initial values $\rho^1 = 0.7$, $\rho^2 = 0.6$ and $\rho^3 = 0.2$ are shown. In this situation more cars are approaching the junction than can enter road 3. We are in the situation of Case 1 with the analytical value $\rho_0^i = \rho_+(\sigma/2) = 0.83536$. Thus the flow in the exiting road is set to its maximum, while there are jams propagating upstream in the ingoing roads. Here we observe only in edge 3 a layer, which interacts with the tail of the rarefaction wave. In the ingoing roads the unstable layer solution enforce the new values at the junction. In these roads the shock waves of the relaxation model are slightly behind those of the macroscopic one. This stems from an initial layer, as the layer at the junction has to form at the beginning, see Figure 5.2. This happens in short time and is not visible at the rarefaction waves, but it remains noticeable at the shocks. The speeds of the shocks is identical in both models, as the connected states coincide, i.e. the delay does not change over time.

In the next example, with the initial values $\rho^1 = 0.05$, $\rho^2 = 0.6$ and $\rho^3 = 0.2$, few

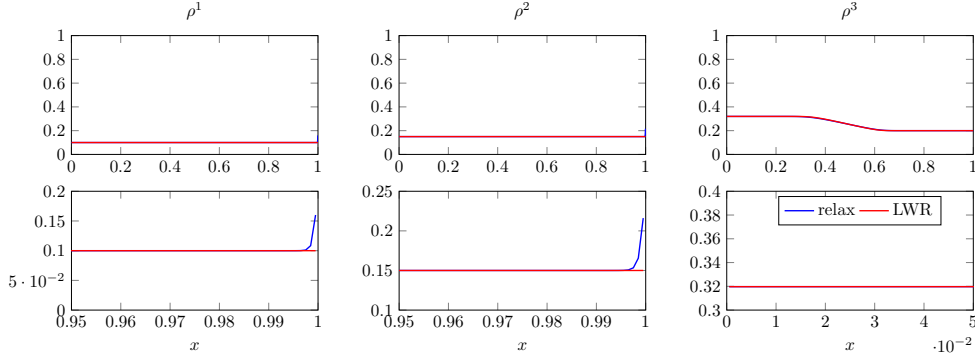


Fig. 6.1: Fair merging with $\rho^1 = 0.1$, $\rho^2 = 0.15$, $\rho^3 = 0.2$. Red: solutions of the LWR-equations, blue: solutions of the relaxation system. First row: solutions on the full domain, second row: zoom around the node.

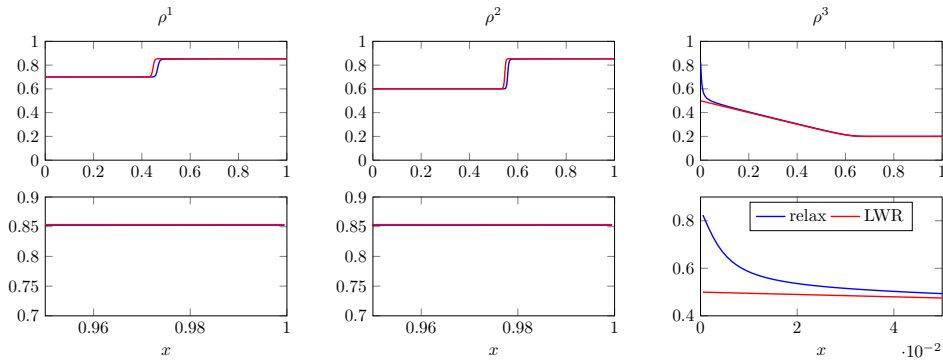


Fig. 6.2: Fair merging with $\rho^1 = 0.7$, $\rho^2 = 0.6$, $\rho^3 = 0.2$.

cars enter from road 1 but many from road 2. We are in Case 4, first subcase. The analytical value at the junction is $\rho_0^i = \rho_+(\sigma - F(\rho_B^1)) = 0.7179$. As shown in Figure 6.3, the flow in road 3 is at maximum such that all cars from road 1 and most of road 2 can pass. Those which do not fit in, create a jam in road 2. Again we see a delay of the shock, as in the previous example. Similarly we observe a layer in edge 3. But here also a layer in road 1 is present, as the solution of the half space is now stable.

REMARK 12. *We mention that the numerical investigation of conditions (3.11) gives slightly different values for the relaxation system at the nodes, but the same results in the interior of the domain. That means, also in this case, the relaxation system leads to the LWR equations on the network with the fair merging condition (3.15).*

6.2. Merging with priority lane. Here, the numerical solutions of the relaxation model with the coupling conditions 3.8 are compared to those obtained for the LWR model with the coupling conditions 3.16.

In the first example with $\rho^1 = 0.6$, $\rho^2 = 0.7$ and $\rho^3 = 0.2$, shown in Figure 6.4,

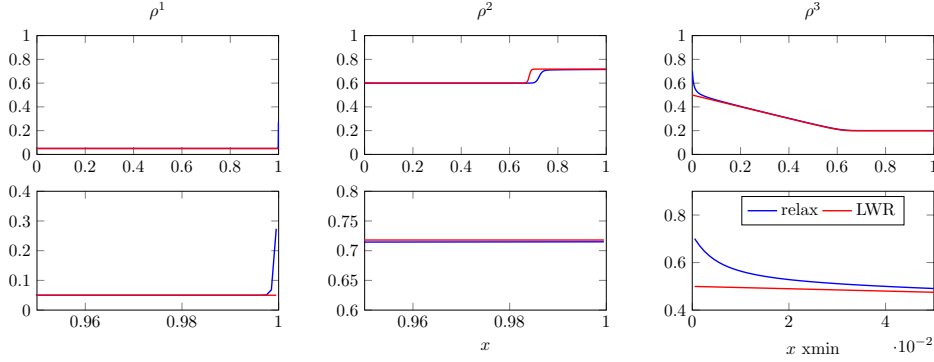


Fig. 6.3: Fair merging with $\rho^1 = 0.05$, $\rho^2 = 0.6$, $\rho^3 = 0.2$.

many cars arrive at the junction. As those of road 1 have priority, the maximal flow

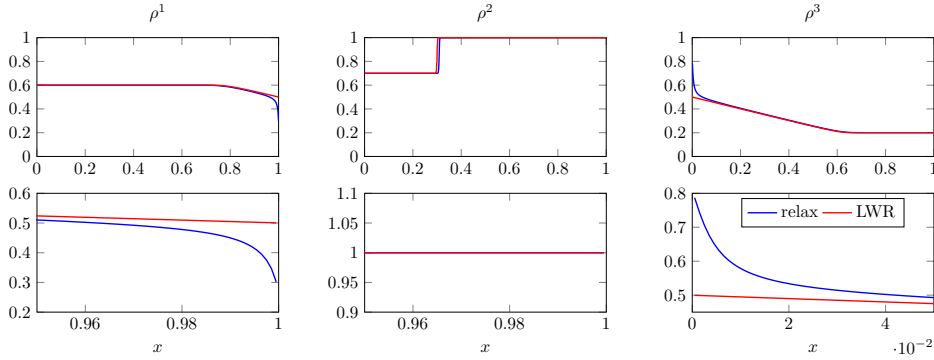


Fig. 6.4: Priority merge with $\rho^1 = 0.6$, $\rho^2 = 0.7$, $\rho^3 = 0.2$.

is established, while all cars in road 2 have to wait. Layers can be observed in road 1 and 3.

In the second example we consider a situation, with the same amount of cars in the ingoing roads and only little space in the outgoing one $\rho^1 = 0.4$, $\rho^2 = 0.4$, $\rho^3 = 0.7$. As expected, we can see in Figure 6.5 that all the cars in road 2 have to wait and thus a larger shock forms. Not all cars in the first road can pass, but the flow is larger as in the second road.

In both cases we obtain a perfect numerical agreement of relaxation solutions and LWR-solutions on the network outside of the layers.

6.3. Diverging with drivers preferences. We consider a junction with equal drivers preferences $\alpha = \frac{1}{2}$ and conditions 3.28 for the macroscopic equations and (3.20), (3.24) for the relaxation problem. We consider two examples. First, with the initial conditions $\rho^1 = 0.8$, $\rho^2 = 0.1$ and $\rho^3 = 0.3$, there is enough space in both outgoing roads such that the maximal flow can be established, as shown in Figure 6.6. In Figure 6.7 the solutions corresponding to the initial values $\rho^1 = 0.6$, $\rho^2 = 0.9$ and $\rho^3 = 0.0$ are shown. Although road 3 is completely free, only few case can enter, as their way is blocked by cars waiting to enter road 2. Thus the high density on road

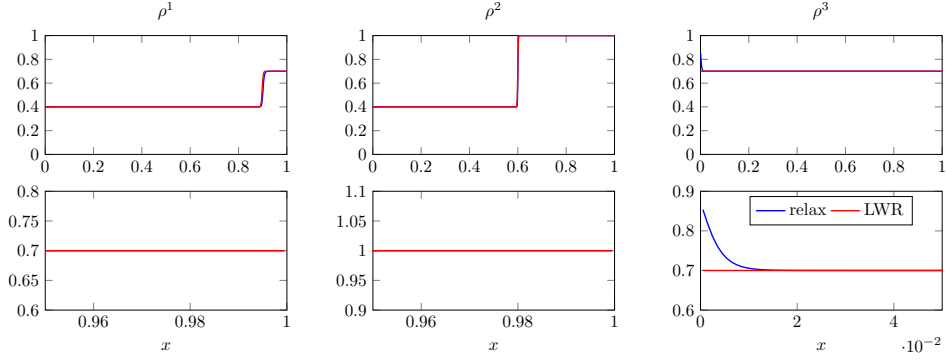


Fig. 6.5: Priority merge with $\rho^1 = 0.4$, $\rho^2 = 0.4$, $\rho^3 = 0.7$.

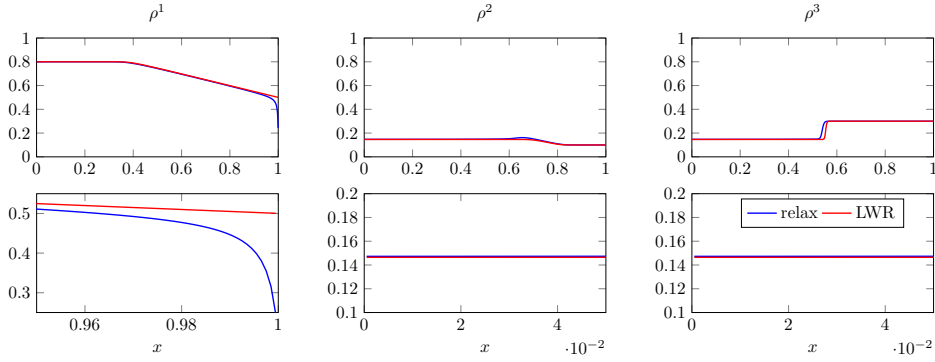


Fig. 6.6: Diverging with driver preferences: $\rho^1 = 0.8$, $\rho^2 = 0.1$, $\rho^3 = 0.3$

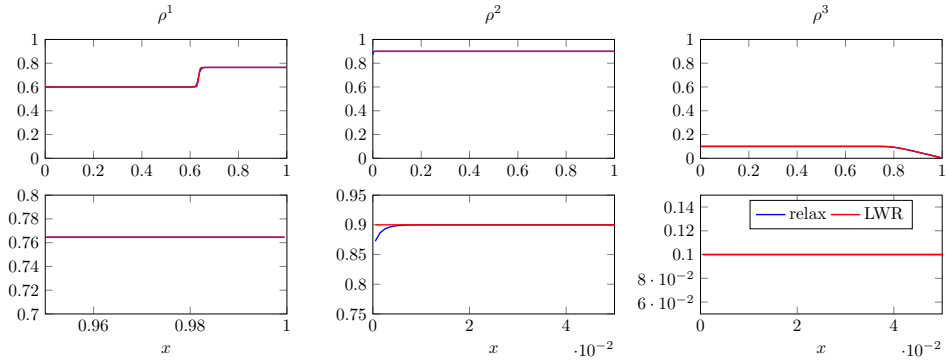


Fig. 6.7: Diverging with driver preferences: $\rho^1 = 0.6$, $\rho^2 = 0.9$, $\rho^3 = 0.0$

2 is causing a left going shock on the ingoing road. A layer forms only on road 2, since on the other two the macroscopic characteristics move away from the junction.

6.4. Diverging without preferences. We consider the situation with condition 3.30 for the macroscopic and conditions 3.22, 3.26 for the relaxation model. The first example investigates the case $\rho^1 = 0.7$, $\rho^2 = 0.2$, $\rho^3 = 0.1$, see Figure 6.8. In this

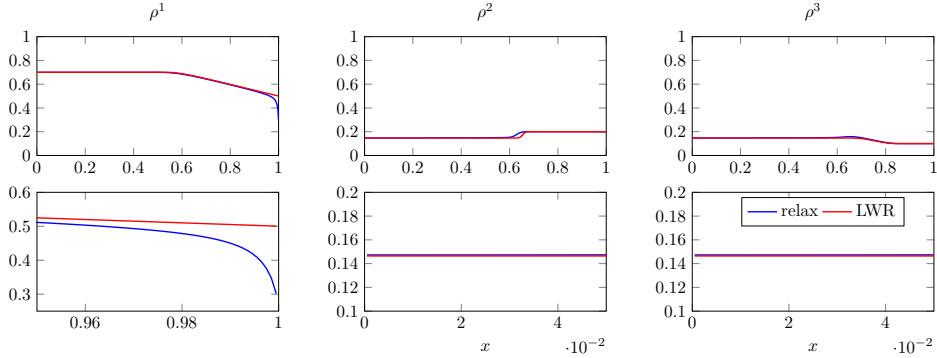


Fig. 6.8: Diverging without preferences: $\rho^1 = 0.7$, $\rho^2 = 0.2$, $\rho^3 = 0.1$.

case, the flux is distributed equally onto the outgoing roads, such that a small shock and a small rarefaction wave arise. On the right hand side we observe that a layer forms in the first road but not in the two exiting ones.

In the second example, Figure 6.9, the results with the initial conditions $\rho^1 = 0.6$, $\rho^2 = 0.1$ and $\rho^3 = 0.95$ are shown. Since the traffic on road 3 is dense only very

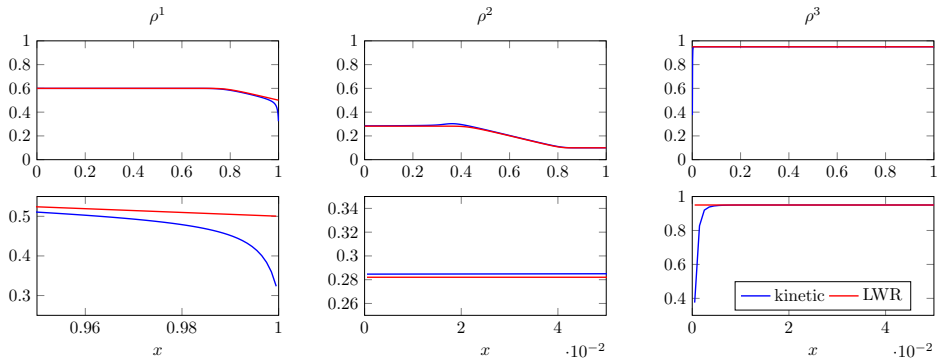


Fig. 6.9: Diverging without preferences: $\rho^1 = 0.6$, $\rho^2 = 0.1$, $\rho^3 = 0.95$

few cars enter there. Most of the vehicles enter into road 2. In the solution of the relaxation model we observe two layers, one interacting with the rarefaction wave on road 1 and one due to the ingoing characteristics on road 3. As for the merging case, we observe a very good numerical agreement between the solutions of the relaxation model and the LWR solution away from the layers at the nodes.

7. Conclusions. We have introduced general coupling conditions for a TLD-relaxation model for LWR-networks. These coupling conditions are related, via an asymptotic analysis at the nodes to well known coupling conditions for the LWR-network.

The asymptotic analysis shows that a classical merge condition for the nonlinear scalar conservation law is related in the zero-relaxation limit to an equal density coupling condition for the relaxation system. The numerical findings support and illustrate the analytical results. One also observes that there is a range of coupling conditions for the relaxation model leading to the same merge condition for the scalar conservation law.

For the case of a diverging junction coupling conditions have been defined respecting the physical invariant domain. They are investigated numerically on the network in the limit as $\epsilon \rightarrow 0$ showing again agreement of the numerical solutions of the relaxation system and the LWR solution for small values of ϵ .

Finally, we remark, that the analytical procedure, presented here for the merging case and a special coupling condition, could be extended to the diverging case or other coupling conditions in the merging case.

REFERENCES

- [1] A. Aw and M. Rascle, *Resurrection of second order models of traffic flow?*, SIAM J. Appl. Math., 60, 916–938, 2000.
- [2] A. Aw, A. Klar, T. Materne, M. Rascle, *Derivation of continuum flow traffic models from microscopic Follow the leader models*, SIAM J. Appl. Math. 63 (1), 259-278, 2002
- [3] D. Aregba-Driollet, V. Milisic, *Kinetic approximation of a boundary value problem for conservation laws*, Numer. Math. 97, 595–633, 2004
- [4] M. Banda, M. Herty, A. Klar, *Gas flow in pipeline networks*, NHM 1(1), 41-56, 2006
- [5] C. Bardos, R. Santos, and R. Sentis, *Diffusion approximation and computation of the critical size*, Trans. Amer. Math. Soc. 284, 2, 617-649, 1984
- [6] N. Bellomo and C. Dogbe, *On the modeling of traffic and crowds: A survey of models, speculations, and perspectives*, SIAM Rev., 53, 409-463, 2011.
- [7] A. Bensoussan, J.L. Lions, and G.C. Papanicolaou, *Boundary-layers and homogenization of transport processes*, J. Publ. RIMS Kyoto Univ. 15, 53-157, 1979
- [8] F. Berthelin, P. Degond, V. Le Blanc, S. Moutari, J. Royer, M. Rascle, *A Traffic-Flow Model with Constraints for the Modeling of Traffic Jams*, Mathematical Models and Methods in Applied Sciences 18, 1269-1298, 2008
- [9] R. Borsche, A. Klar, *A nonlinear discrete velocity relaxation model for traffic flow*, SIAM J. Appl. Math. 78, 5, 2891-2917, 2018
- [10] R. Borsche, A. Klar, *Kinetic layers and coupling conditions for scalar equations on networks*, Nonlinearity, 31, 7, 3512-3541, 2018
- [11] R. Borsche, A. Klar, *Kinetic layers and coupling conditions for macroscopic equations on networks I: The wave equation*, SIAM J. Sci. Comput. 40, 3, A1784-A1808, 2018.
- [12] R. Borsche, A. Klar, J.Kall, T.N.H. Pham, *Kinetic and related macroscopic models for chemotaxis on networks*, M3AS, 26, No. 6, 1219-1242, 2016
- [13] G. Bretti, R. Natalini, M. Ribot, *A hyperbolic model of chemotaxis on a network: a numerical study*, ESAIM Math. Model. Numer. Anal., 48(1) ,231–258, 2014.
- [14] G.M. Coclite, M. Garavello, B. Piccoli, *Traffic flow on a road network*, SIAM J. Math. Anal. 36, 6, 1862-1886, 2005.
- [15] R.M. Colombo, M. Garavello, *On the Cauchy problem for the p-system at a junction*, SIAM J. Math. Anal., 39, 1456–1471 2008.
- [16] R.M. Colombo, R.,C. Mauri, *Euler system for compressible fluids at a junction*, J. Hyperbolic Differ. Equ., 5(3), 547–568, 2008.
- [17] A. Corli, L. di Ruvo, L. Malaguti, M. D. Rosini, *Traveling waves for degenerate diffusive equations on networks*, NHM 12,3, 339 - 370, 2017.
- [18] F. Coron, F. Golse, C. Sulem, *A Classification of Well-posed Kinetic Layer Problems*, CPAM, Vol. 41, 409, 1988.
- [19] C. F. Daganzo, *A behavioral theory of multi-lane traffic flow part I: Long homogeneous freeway sections*, Trans. Res. B, 36 (2002), pp. 131–158
- [20] C. F. Daganzo, *A behavioral theory of multi-lane traffic flow part II: Merges and the onset of congestion*, Trans. Res. B, 36 (2002), pp. 159–169.
- [21] L. Fermo and A. Tosin, *A fully-discrete-state kinetic theory approach to modeling vehicular traffic*, SIAM J. Appl. Math., 73, 1533-1556, 2013.

- [22] M. Garavello, *A review of conservation laws on networks* NHM 5, 3, 565 - 581, 2010
- [23] M. Garavello and B. Piccoli, *Traffic flow on a road network using the Aw-Rascle model*, Comm. Partial Differential Equations, 31 (2006), pp. 243–275.
- [24] M. Garavello, B. Piccoli, *Traffic flow on networks*, AIMS Series on Applied Mathematics, 1, American Institute of Mathematical Sciences (AIMS), Springfield, 2006
- [25] F. Golse, *Analysis of the boundary layer equation in the kinetic theory of gases*, Bull. Inst. Math. Acad. Sin. 3, 1, 211-242, 2008
- [26] J. M. Greenberg, *Extensions and amplifications of a traffic model of Aw and Rascle model*, SIAM J. Appl. Math., 62, 729–745, 2002.
- [27] D. Helbing, *Gas-kinetic derivation of Navier-Stokes-like traffic equation*, Physical Review E, 53 (1996), pp. 2366–2381.
- [28] M. Herty and S. Moutari, *A macro-kinetic hybrid model for traffic flow on road networks*, Comput. Methods Appl. Math., 9, 3,238–252, 2009.
- [29] M. Herty, M. Rascle, *Coupling conditions for a class of second order models for traffic flow*, SIAM Math. Anal. 38, 2, 595–616, 2006.
- [30] M. Herty and A. Klar, *Modeling, simulation, and optimization of traffic flow networks*, SIAM J. Sci. Comput., 25 (2003), pp. 1066–1087.
- [31] M. Herty, G. Puppo, S. Roncoroni, G. Visconti, *The BGK approximation of kinetic models for traffic*, Kinetic & Related Models 13, 279, 2020.
- [32] H. Holden, N.H. Risebro, *A mathematical model of traffic flow on a network of unidirectional roads*, SIAM J. Math. Anal. 26, 4, 999–1017, 1995.
- [33] A. Klar and R. Wegener, *Enskog-like kinetic models for vehicular traffic*, J. Stat. Phys., 87 , 91-114, 1997.
- [34] A. Klar, R. Wegener, *Kinetic Derivation of Macroscopic Anticipation Models for Vehicular Traffic*, SIAM J. Appl. Math. 60 (5), 1749-1766, 2000.
- [35] O. Kolb, G. Costeseque, Goatin, Göttlich, *Pareto-optimal coupling conditions for the Aw-Rascle-Zhang traffic flow model at junctions*, SIAM Appl. Math. 78, 4 1981-2002, 2018
- [36] J. P. Lebacque, *Les modeles macroscopiques du trafic*, Annales des Ponts, 67 (1993), pp. 28–45.
- [37] G. Leugering, Guenter, E.J.P.G. Schmidt, *On the modelling and stabilization of flows in networks of open canals*, SIAM J. Control Optim., 41(1), 164–180 2002.
- [38] J.-G. Liu, Z. Xin, *Boundary-layer behavior in the fluid-dynamic limit for a nonlinear model Boltzmann Equation*, Arch. Rational Mech. Anal. 135, 61-105, 1996.
- [39] R. Natalini, A. Terracina, *Convergence of a relaxation approximation to a boundary value problem for conservation laws*, Comm. Partial Differential Equations, 26(7-8), 1235–1252, 2001.
- [40] A. Nouri, A. Omrane, J.P. Vila, *Boundary conditions for scalar conservation laws from a kinetic point of view*. J. Statist. Phys., 94(5-6), 779–804, 1999.
- [41] H. Payne, *FREFLO: A macroscopic simulation model of freeway traffic*, Transportation Res. Record, 722 (1979), pp. 68–75.
- [42] G. Puppo, M. Semplice, A. Tosin, G. Visconti, *Kinetic models for traffic flow resulting in a reduced space of microscopic velocities*, Kinet. Relat. Models 10(3), 823–854, 2017.
- [43] S. Ukai, T. Yang, and S.-H. Yu, *Nonlinear boundary layers of the Boltzmann equation. I. Existence*, Comm. Math. Phys. 236, 3, 373-393, 2003.
- [44] W.-C. Wang, Z. Xin, *Asymptotic limit of initial boundary value problems for conservation laws with relaxational extensions*, Communications on Pure and Applied Mathematics, 51,5 505–535, 1998.
- [45] W.-Q. Xu, *Boundary conditions and boundary layers for a multi-dimensional relaxation model*, Journal of Differential Equations 197, 1, 10, 85-117, 2004.
- [46] W.-A. Yong, *Boundary conditions for hyperbolic systems with stiff relaxation*, Indiana University Mathematics Journal 48, 1, 115-137, 1999